Supporting Information

Exploring allosteric properties of mammalian ALOX15: octyl (N-(4-(benzofuran-2-yl)-2-methoxyphenyl)sulfamoyl)- and octyl (N-(4-(1H-indol-2-yl)-2-methoxyphenyl)sulfamoyl)carbamates as ALOX inhibitors

Authors: Viktor Gavrilyuk[a], Alejandro Cruz[b], Vladislav Aksenov[a], Danila Nurgaliev[a], Alexander Zhuravlev[a], Alexey Golovanov[a], José M. Lluch[c], Hartmut Kuhn[d], Igor Ivanov[a]* and Àngels González-Lafont[c]*

Affiliations:

[a] Lomonosov Institute of Fine Chemical Technologies, MIREA - Russian Technological University, Vernadskogo pr. 86, 119571 Moscow, Russia; viktor_gavril@inbox.ru (V.G.); aksenov.v.v@edu.mirea.ru (V.A); alekszhur95@yandex.ru (A.Z.); ivanov_i@mirea.ru (I.I.)

[b] Department of Chemical Engineering-ETSEIB, Universitat Politècnica de Catalunya, 08028, Barcelona, Spain; alejandro.cruz.saez@upc.edu (A.C.)

[c] Departament de Química, Universitat Autònoma de Barcelona, 08193 Bellaterra, Barcelona, Spain; JoseMaria.Lluch@uab.cat (J.M.L.); Angels.Gonzalez@uab.cat (A.G.-L.)

[d] Department of Biochemistry, Charite - University Medicine Berlin, Corporate member of Free University Berlin, Humboldt University Berlin and Berlin Institute of Health, Charitéplatz 1, D-10117 Berlin, Germany; hartmut.kuehn@charite.de

*Correspondence, angels.gonzalez@uab.cat ; ivanov_i@mirea.ru

Tables

Table S1. Most significant interactions that compound **3** forms in the last structure of the MD simulation for the 3:ALOX15 complex. All interacting partners belong to monomer A unless otherwise indicated (A) The main interactions of the representative structure of the most populated cluster for compound **1**, obtained previously after MD simulation*

Group	Type of interaction	Interaction partner	Distance
A 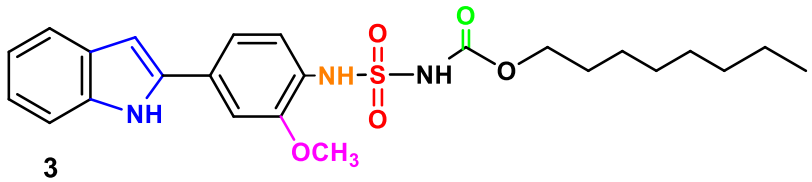 **3**			
NH	hydrogen bond	Ile400 (backbone O)	d (H5-O-Ile 400) = 1.945 Å
OCH_3	electrostatic	Asn193(B) (sidechain NH_2)	d(O1-HD22-Asn 193) = 4.377 Å
NH	hydrogen bond hydrogen bond	Leu192(B) (backbone O) Arg403 (sidechain NH_2)	d(H13-O-Leu192(B)) = 1.887 Å d(N2-HH12-Arg403) = 3.428 Å
SO_2	hydrogen bond hydrogen bond	Asn193(B) (sidechain NH_2) Arg403 (sidechain NH_2)	d(O2-HD22-Asn193) = 3.213 Å d(O3-HH11-Arg403) = 1.691 Å
COO	electrostatic electrostatic	Asn193(B) (sidechain NH_2) Asn193(B) (sidechain NH_2)	d(O4-HD22-Asn193) = 3.103 Å d(O5-HD22-Asn193) = 3.409 Å
B* 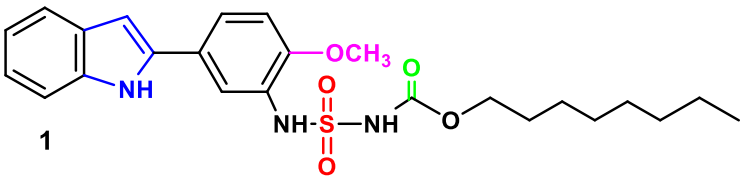 **1**			
NH	hydrogen bond	Fe(III)-OH^-	d(H1-OH) = 2.116 Å
OCH_3	hydrogen bond electrostatic	Gln596 (sidechain NH_2) Arg403 (sidechain NH_2) Arg599	d(O1-HE22-Gln596) = 3.534 Å d(O1-HH11-Arg403) = 4.465 Å **
SO_2	hydrogen bond	Gln596 (sidechain NH_2)	d(O2-HE21-Gln596) = 2.059 Å
COO	hydrogen bond	Leu408 (backbone NH)	d(O4-H-Leu408) = 2.345 Å

* doi: 10.3390/molecules28145418, doi: 10.1021/acs.jmedchem.1c01563

numerous electrostatic interactions of Arg599 sidechain with the MeO group of compound **1.

Figures

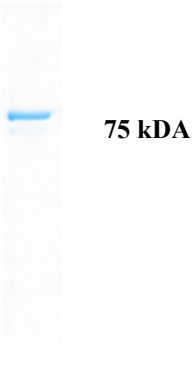

Figure S1. 10% SDS-PAGE electrophoresis of purified rabbit ALOX15.

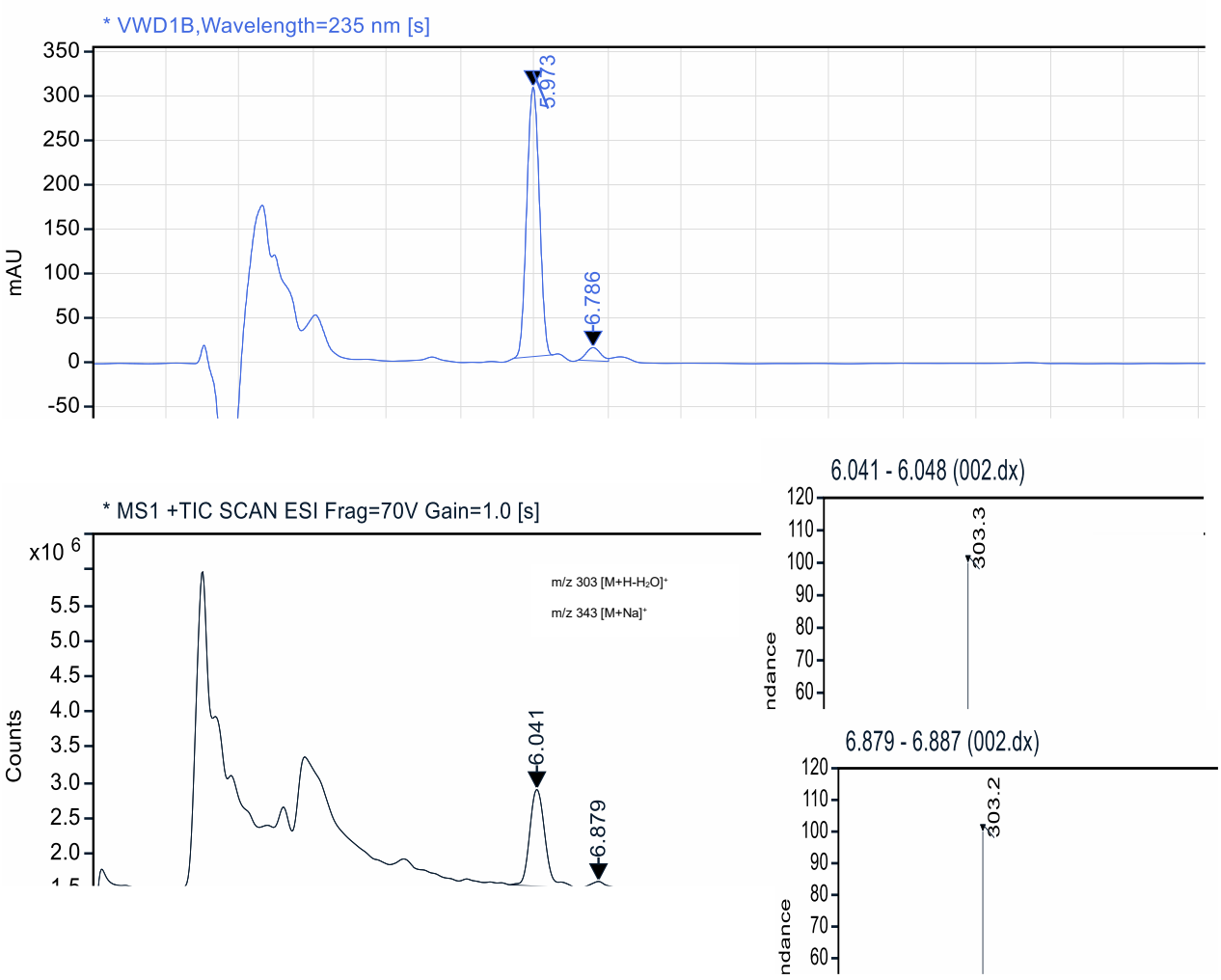

Figure S2. HPLC-MS (UV/MS detection) analysis of AA oxygenation products formed during the incubation with purified ALOX15. A mixture of 25 µM AA and purified rabbit ALOX15 (5µg) in 1 mL PBS was incubated for 3 min at 25 °C. The reaction was stopped by the addition of NaBH4. The sample was acidified, protein was precipitated by the addition of 0.5 mL of acetonitrile, and the precipitate was spun down. The ALOX products were analyzed by HPLC using a Nucleodur C18 Gravity column (Macherey-Nagel, Duüren, Germany; 250 mm × 4 mm, 3 µm particle size) coupled with a guard column (8 ×4 mm, 3 µm particle size) at a flow rate of 1 mL/min. Mass spectra (ESI) were recorded on Agilent 6160 (Agilent, Singapore) either in the positive or negative ionization modes. The mass spectrometer and source parameters were set up as follows: capillary voltage 3.5 kV and 4 kV for positive and negative ionization, respectively; source temperature 65°C; desolvation temperature 350°C; and flow rate of desolvation gas 600 L/h.

A

Michaelis-Menten Best-fit values	no inhibitor	0.5 μM **2**	1.4 μM **2**
k_{cat}	19.10±1.64	9.89±1.09	5.76±0.52
K_M	32.30±5.24	30.54±7.29	26.08±5.86

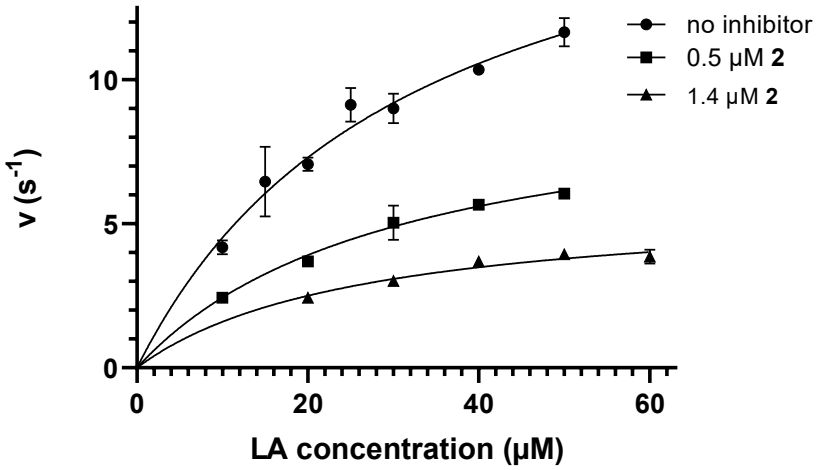

B

Michaelis-Menten Best-fit values	no inhibitor	2.5 μM **2**	14 μM **2**
k_{cat}	4.86±1.02	4.24±0.29	4.13±2.54
K_M	16.14±7.32	19.11±2.52	61.12±18.47

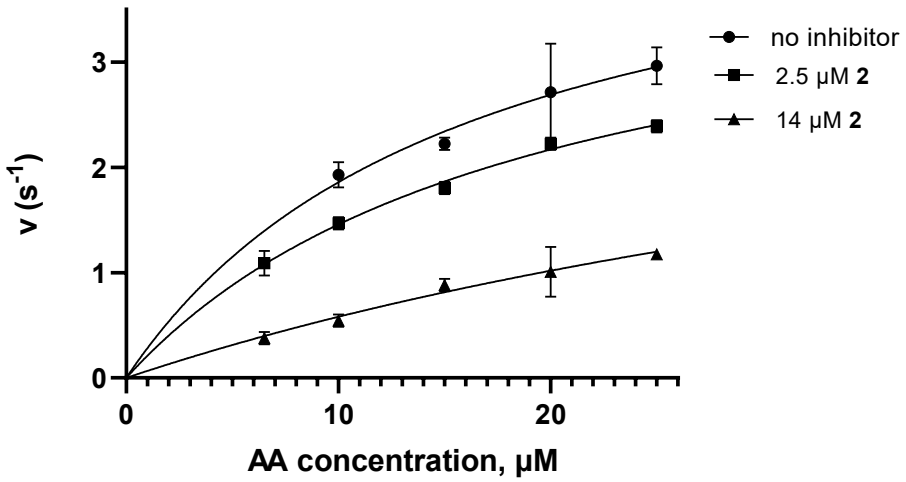

Figure S3. Inhibition of LA (A) and AA (B) oxygenation by rabbit ALOX15 in the presence of compound **2**.

A

Michaelis-Menten Best-fit values	no inhibitor	8 μM **3**	30 μM **3**
k_{cat}	18.83±2.33	9.45±0.71	4.07±0.61
K_M	31.58±7.03	16.49±3.14	9.06±2.57

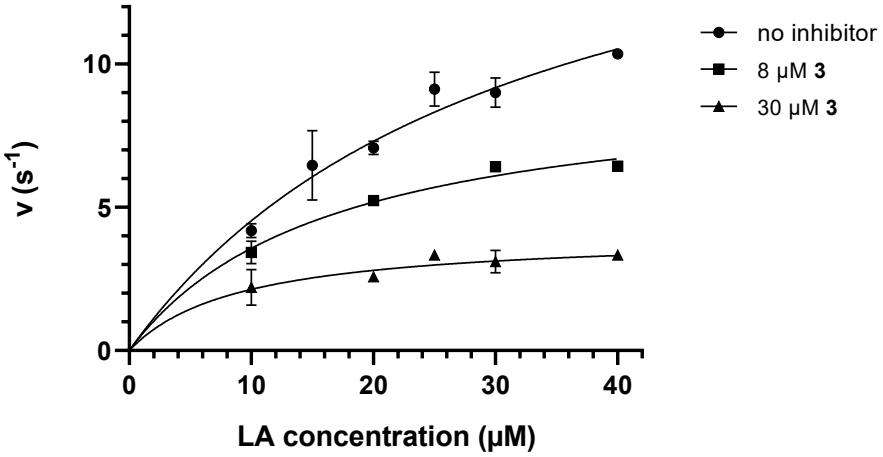

B

Michaelis-Menten Best-fit values	no inhibitor	8 μM **3**	30 μM **3**
k_{cat}	3.96±0.46	3.59±0.41	1.25±0.21
K_M	14.83±3.63	14.77±3.62	5.18±1.95

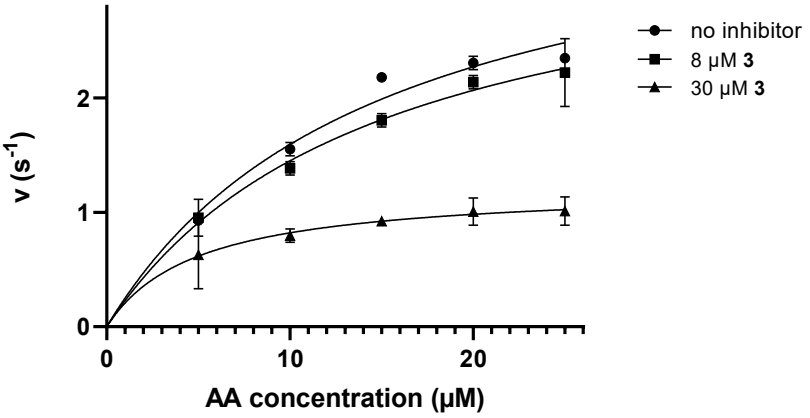

Figure S4. Inhibition of LA (A) and AA (B) oxygenation by rabbit ALOX15 in the presence of compound **3**.

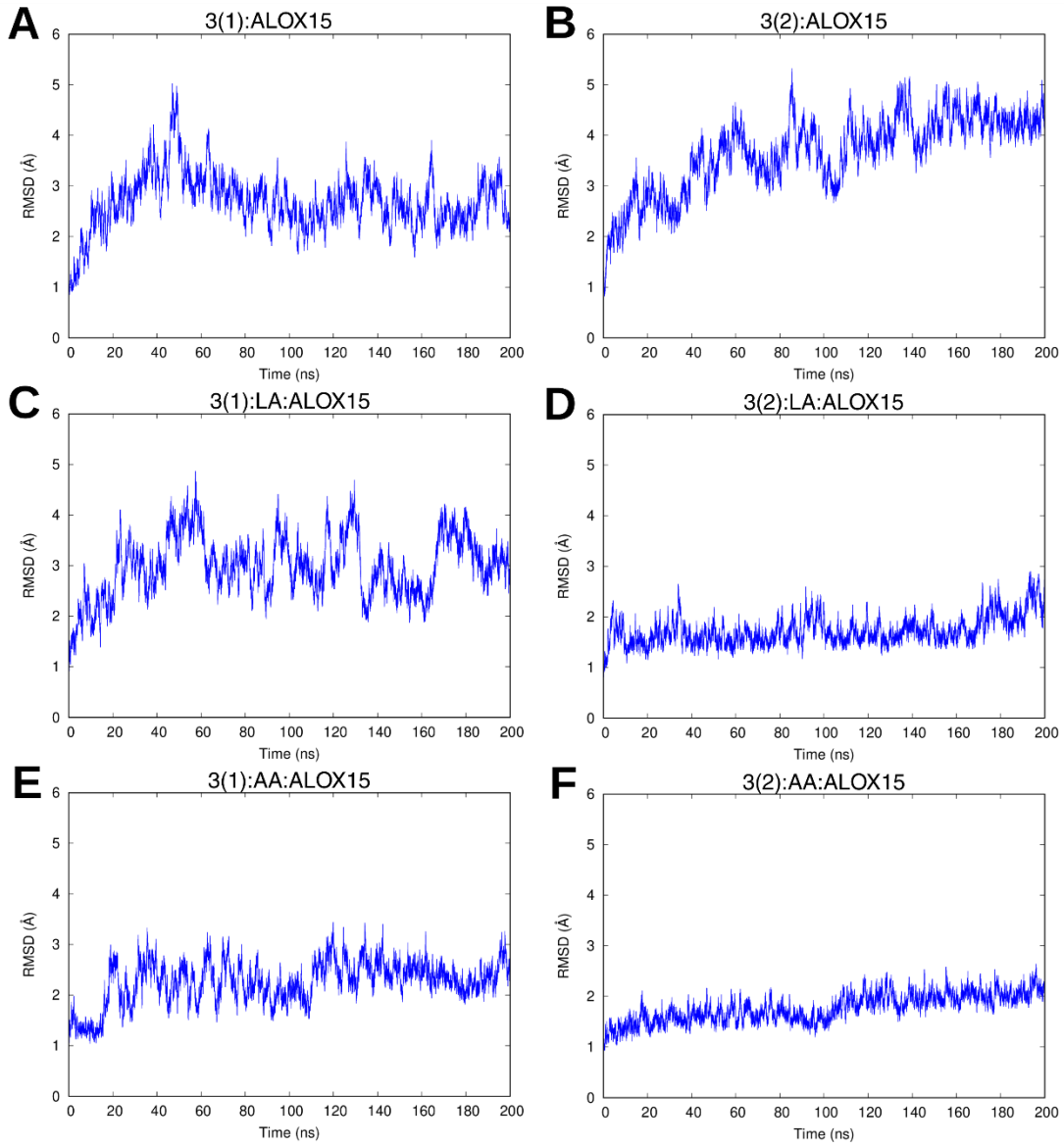

Figure S5. RMSD of the ALOX15 dimer backbone atoms for the different systems. (A) RMSD of 3(1):ALOX15 complex. (B) RMSD of 3(2):ALOX15 complex. (C) RMSD of 3(1):LA:ALOX15 complex. (D) RMSD of 3(2):LA:ALOX15 complex. (E) RMSD of 3(1):AA:ALOX15 complex. (F) RMSD of 3(2):AA:ALOX15 complex.

The backbone RMSD plots of the different complexes demonstrate that the simulations reached convergence during the MD trajectories. In the case of the 3(2):LA/AA:ALOX15 complexes the substrates diminish the RMSD values of the 3(2):ALOX15 complexes. The higher RMSD values in the 3(1):LA/AA:ALOX15 complexes can be attributed to the substrate in the cavity of monomer B that triggers the conversion of the binding mode of inhibitor **3** in **3**(1):ALOX15 complex to that of **3**(2):ALOX15 complex through an inwards movement of α18 helix of monomer A.

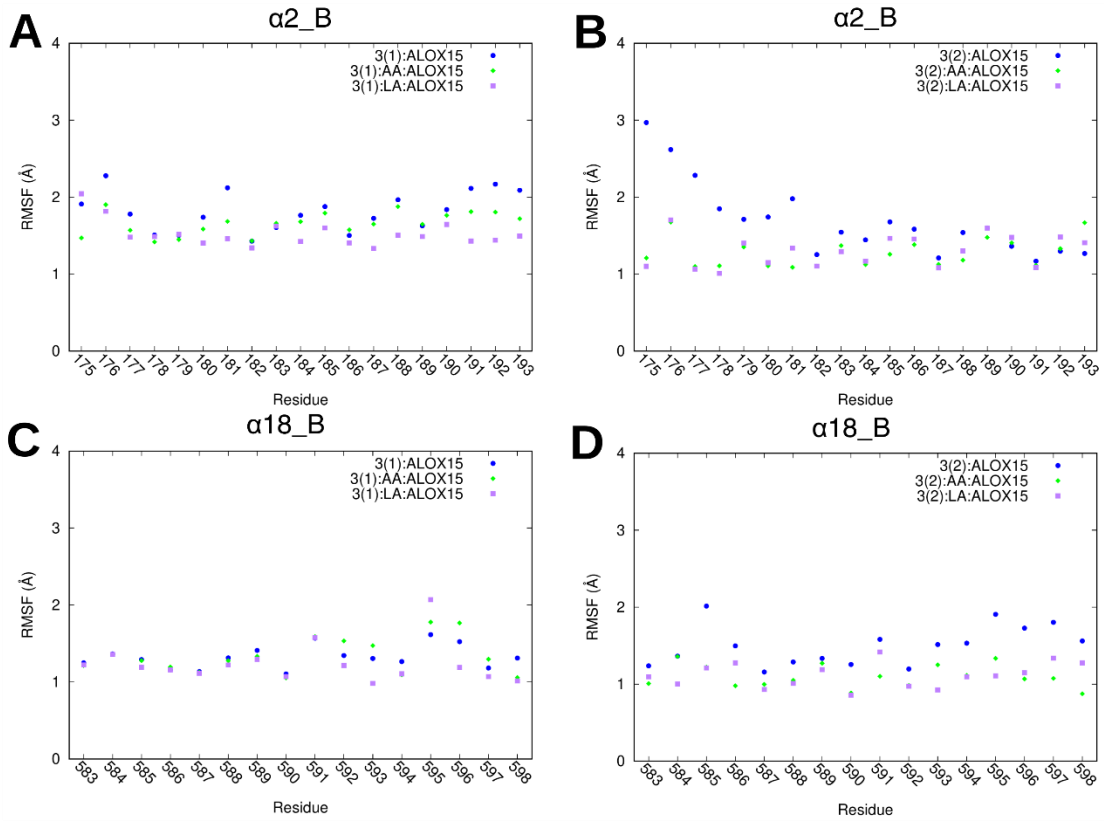

Figure S6. RMSF by residue of helices α2 (Panels A and B) and α18 (Panels C and D) of the ALOX15 monomer B for the different systems.

Analytical data

1-(4-methoxy-3-nitrophenyl)ethan-1-one oxime **(5)**

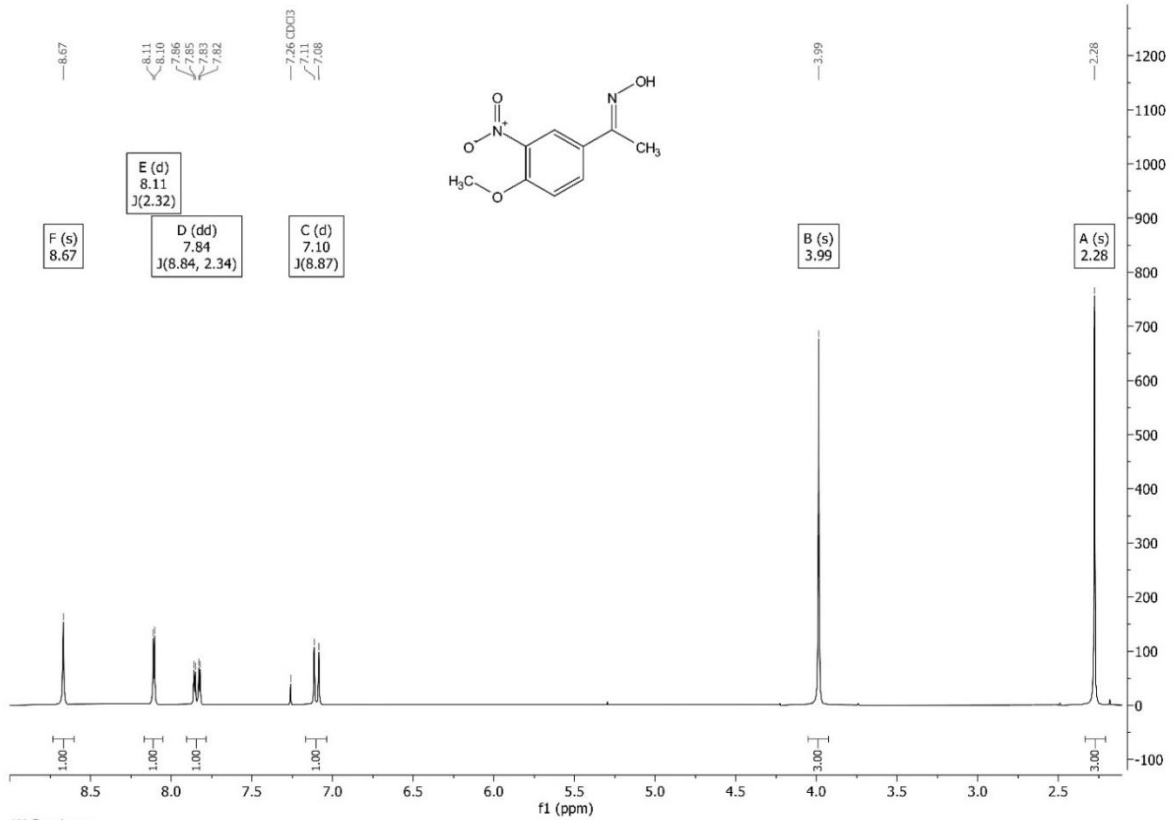

^{1}H NMR spectrum of **5**

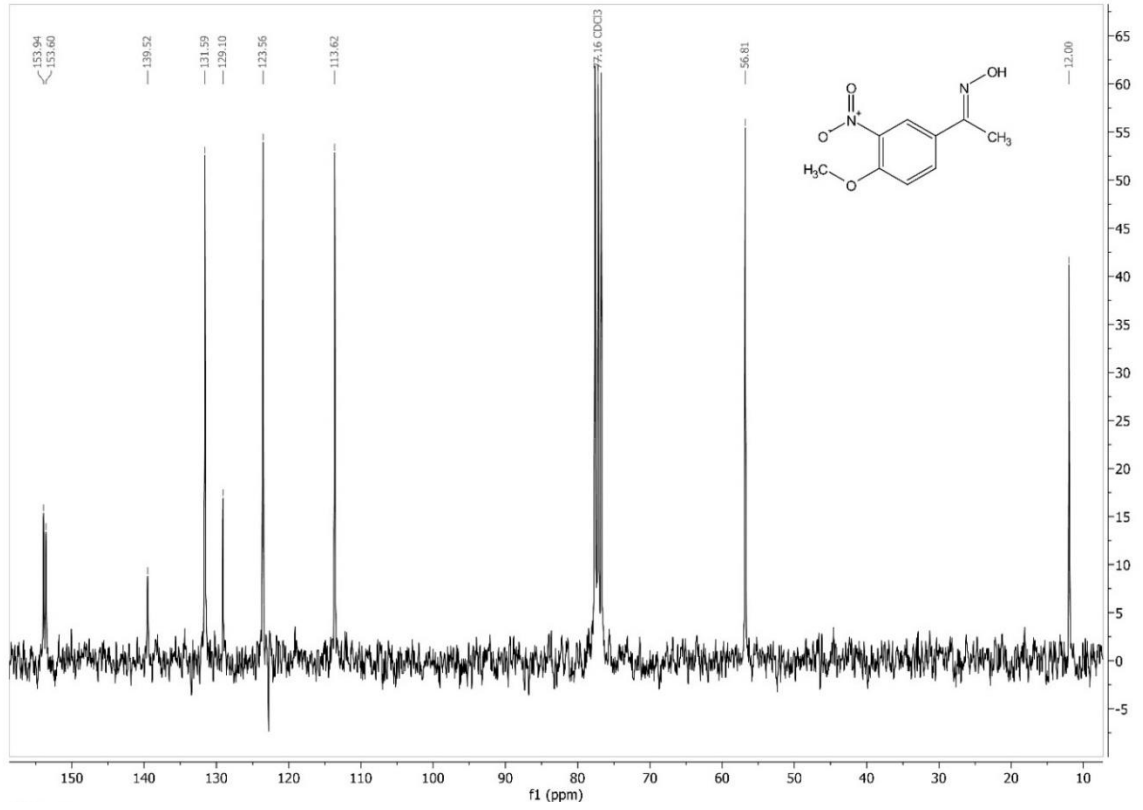

^{13}C NMR spectrum of **5**

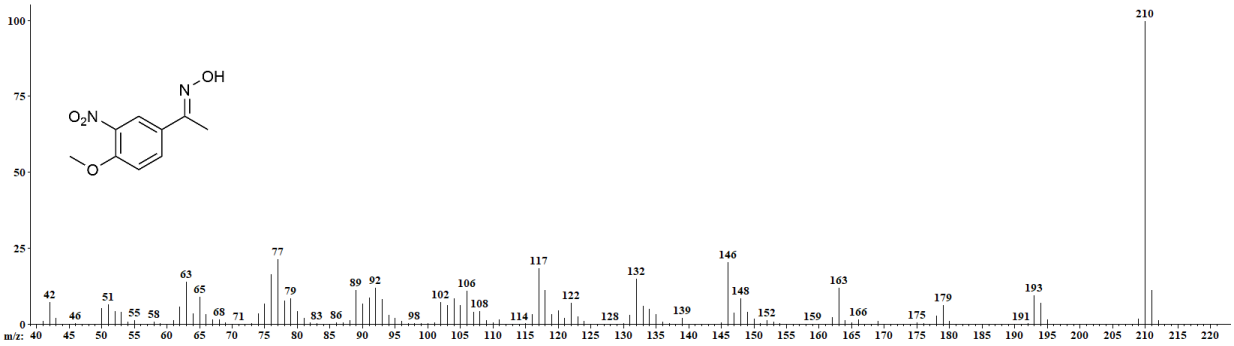

MS spectrum of **5**

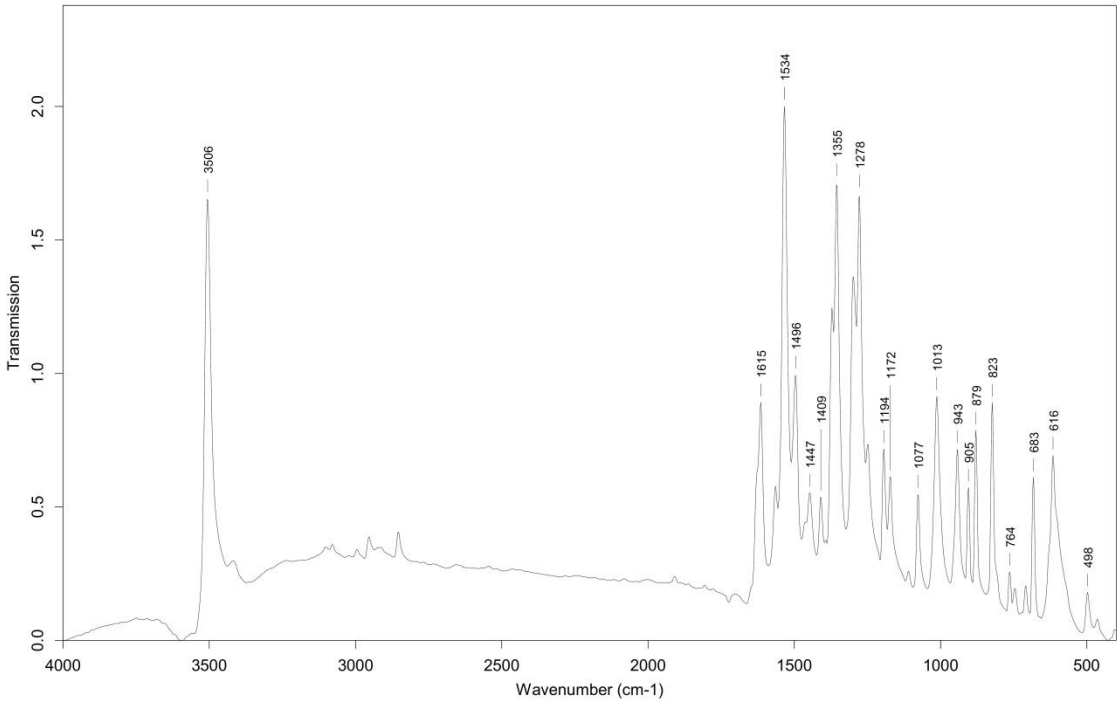

IR spectrum of **5**

***Diphenyliodonium triflate* (6)**

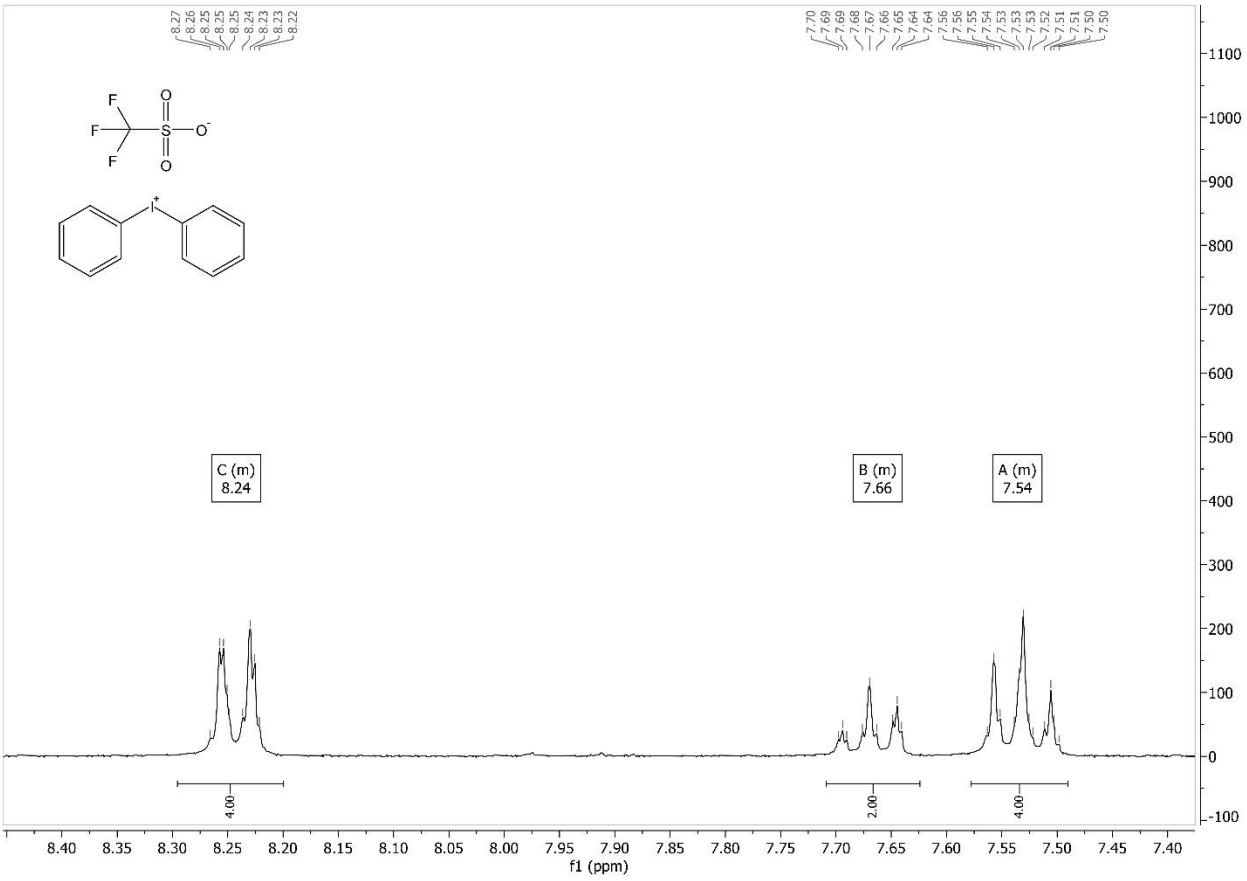

^{1}H NMR spectrum of **6**

***1-(4-methoxy-3-nitrophenyl)ethan-1-one O-phenyl oxime* (7)**

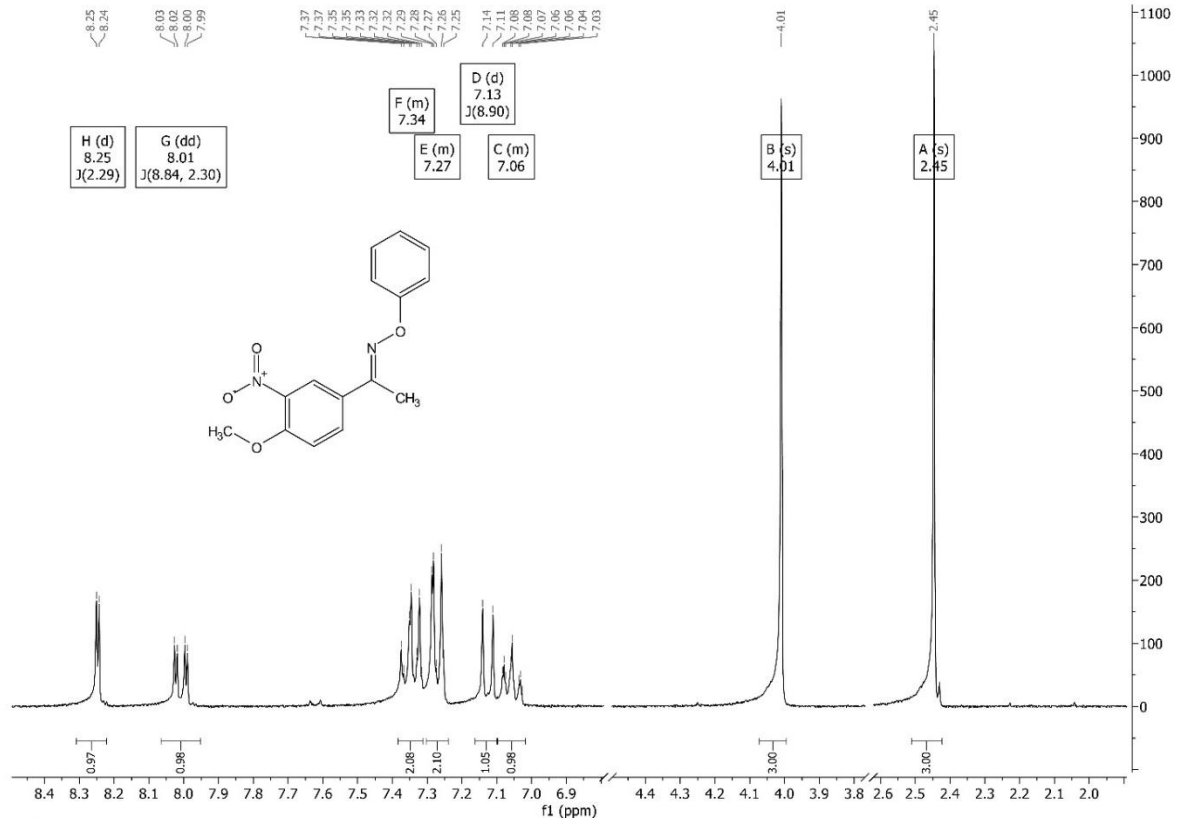

^{1}H NMR spectrum of **7**

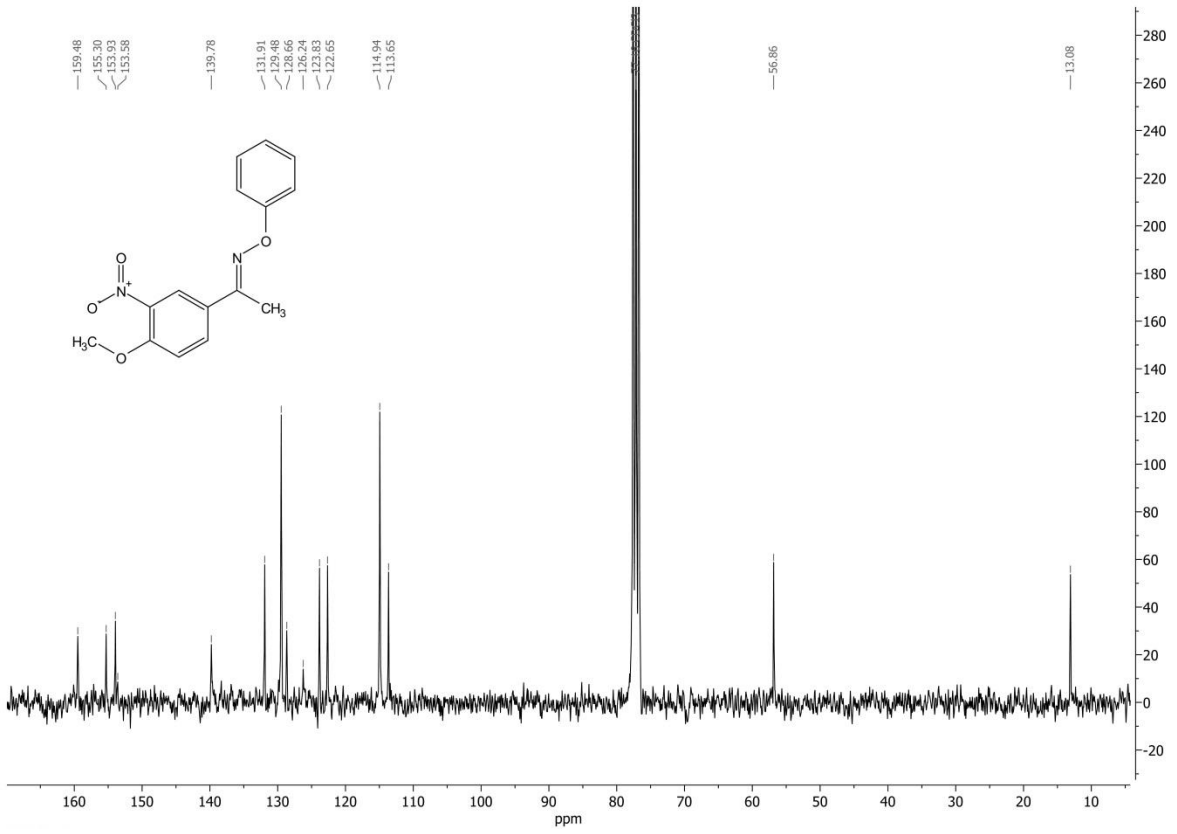

^{13}C NMR spectrum of **7**

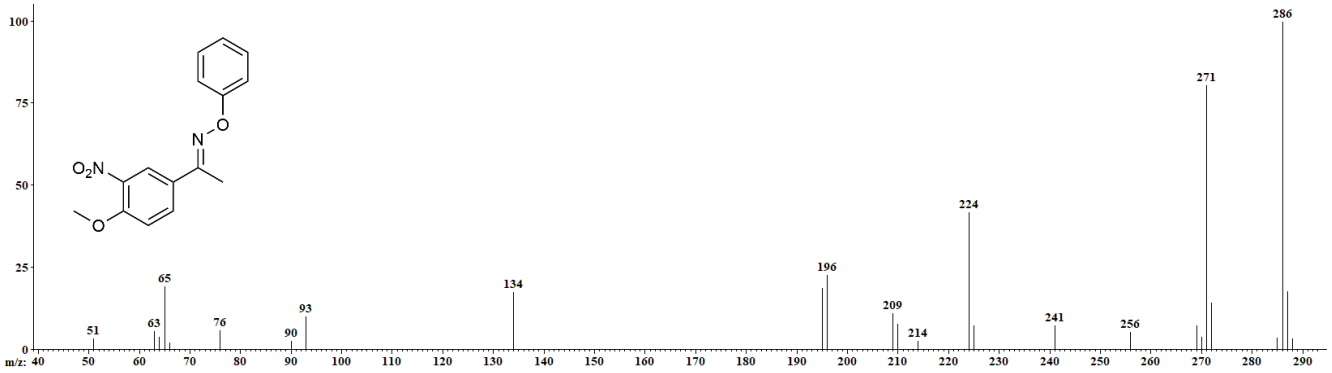

MS spectrum of **7**

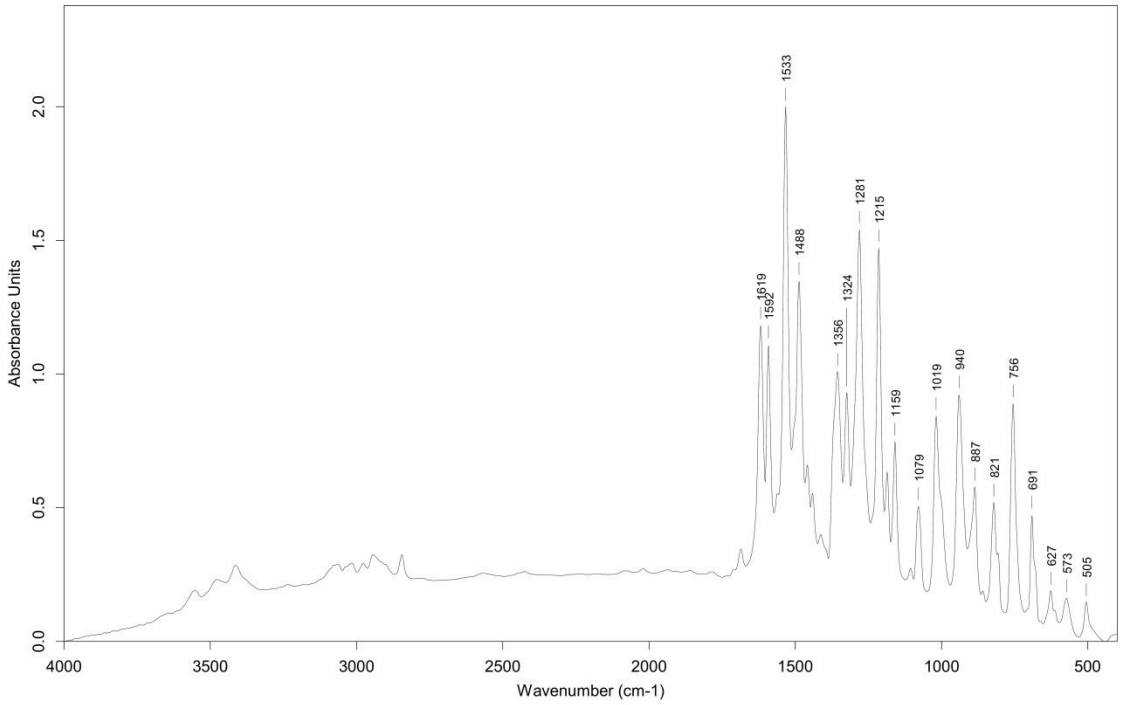

IR spectrum of **7**

***2-(4-methoxy-3-nitrophenyl)benzofuran* (8)**

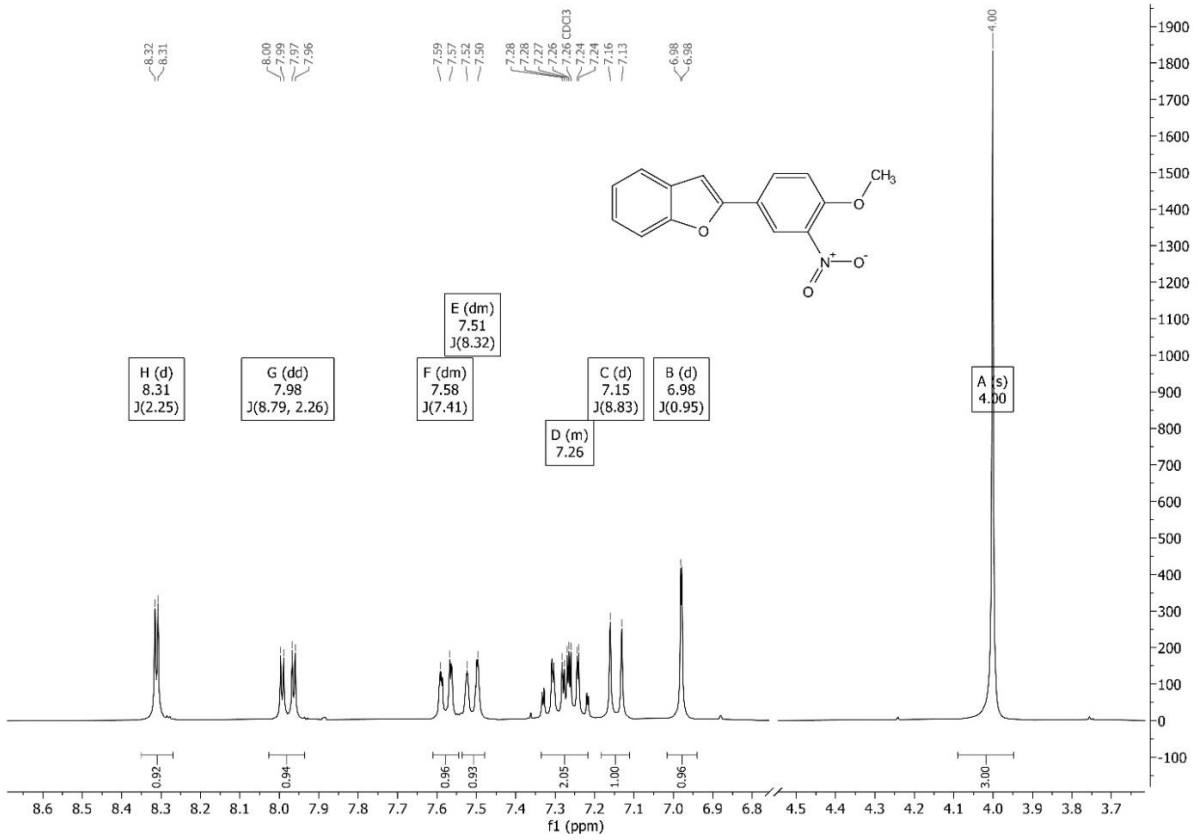

[1]H NMR spectrum of **8**

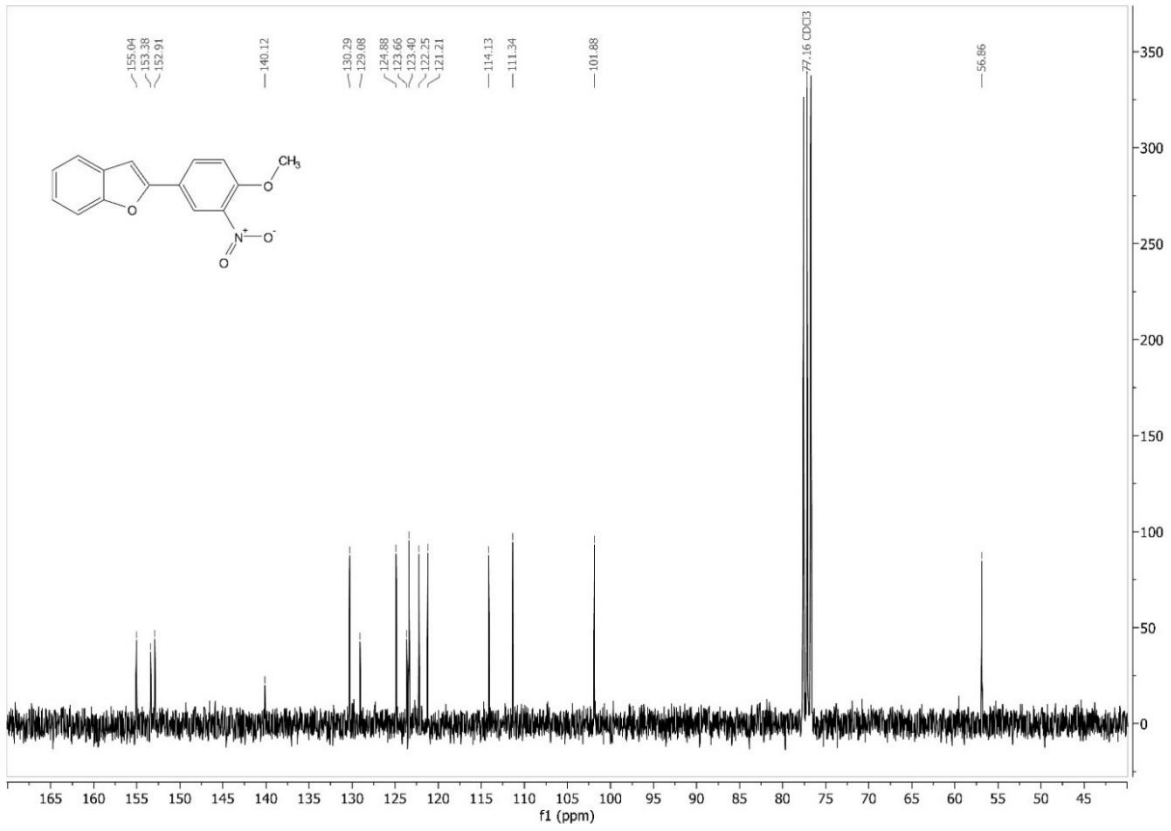

[13]C NMR spectrum of **8**

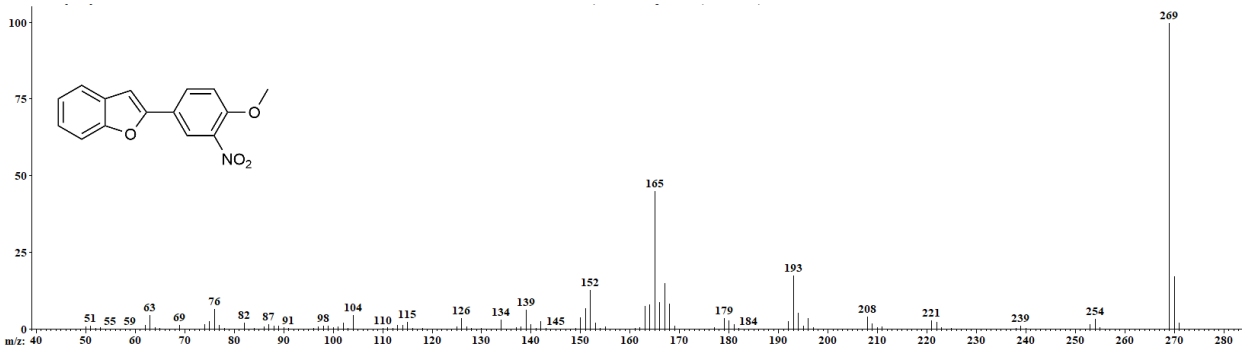

MS spectrum of **8**

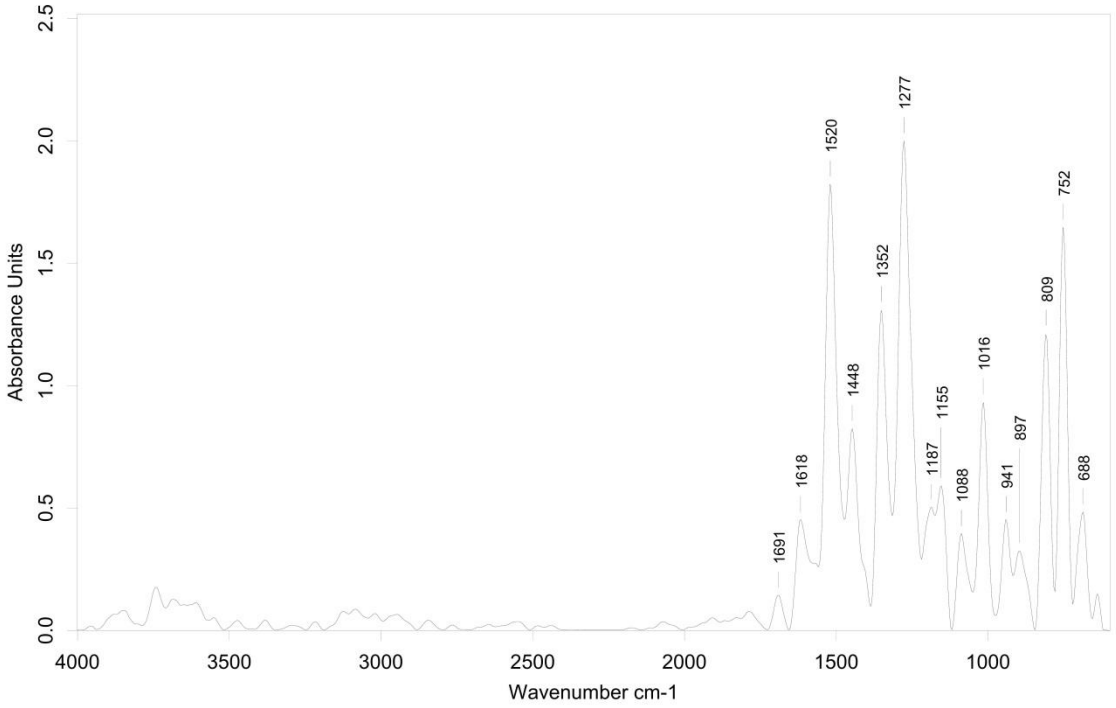

IR spectrum of **8**

***2-(3-amino-4-methoxyphenyl)benzofuran* (9)**

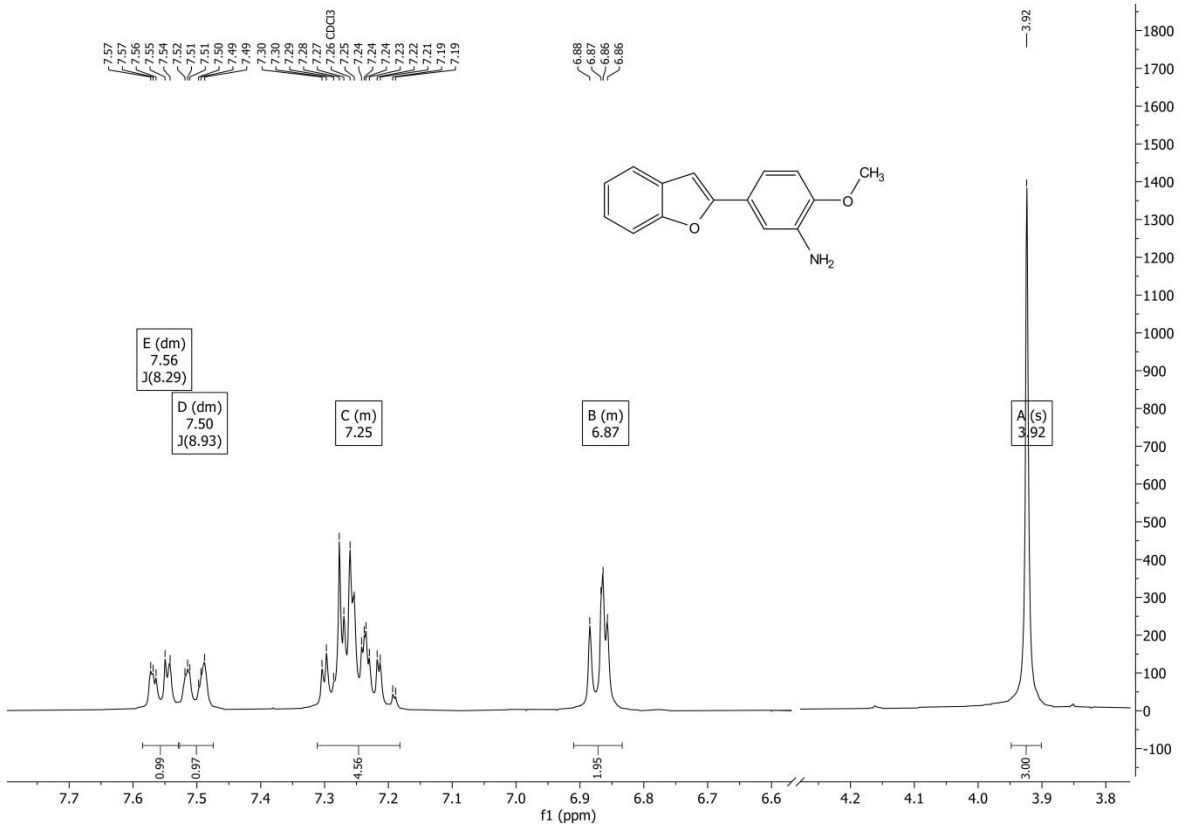

^{1}H NMR spectrum of **9**

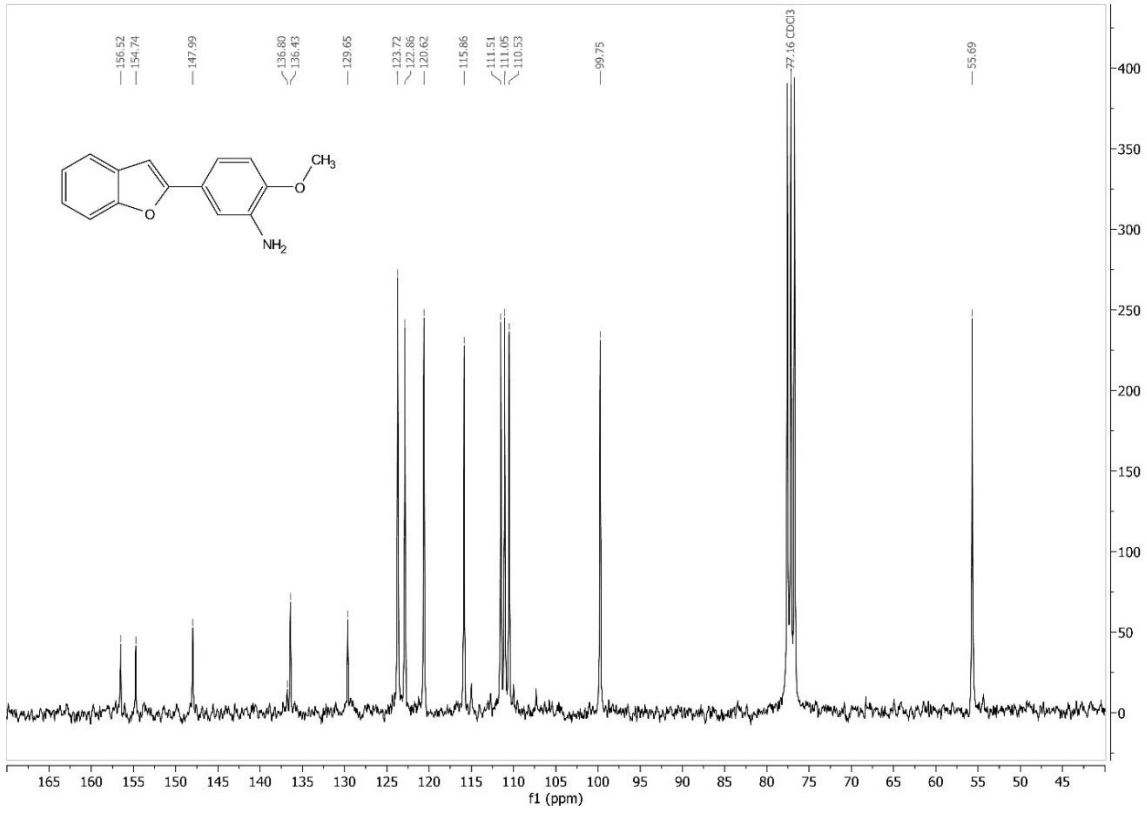

^{13}C NMR spectrum of **9**

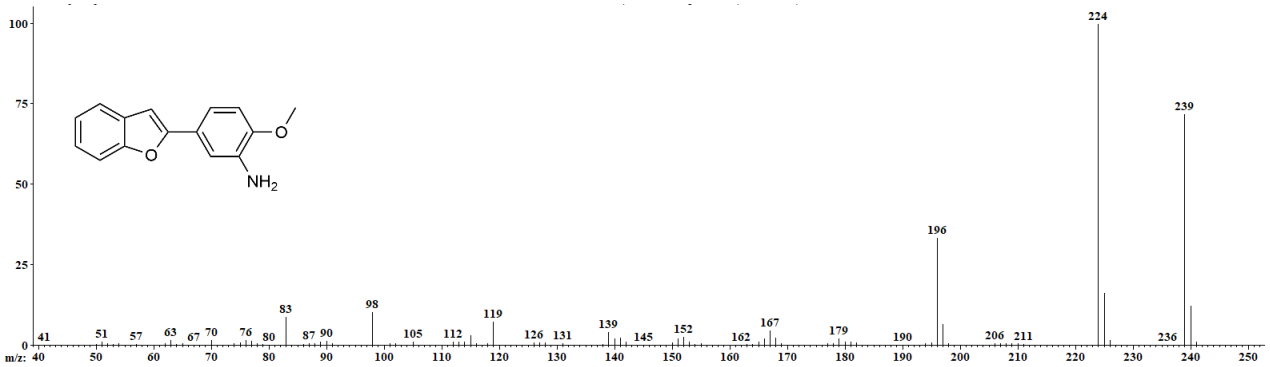

MS spectrum of **9**

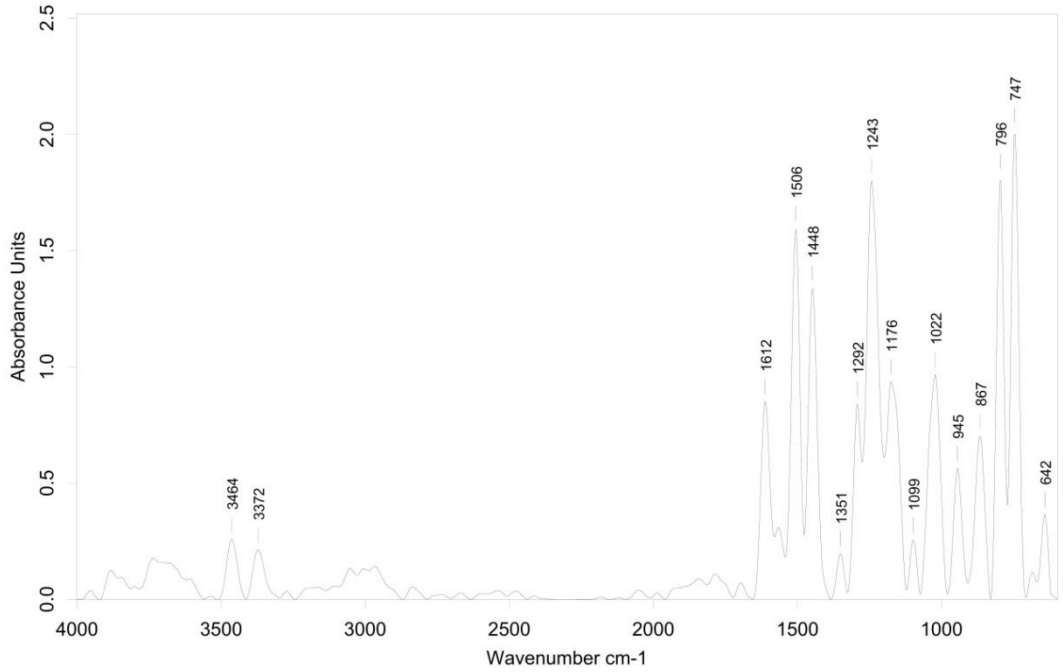

IR spectrum of **9**

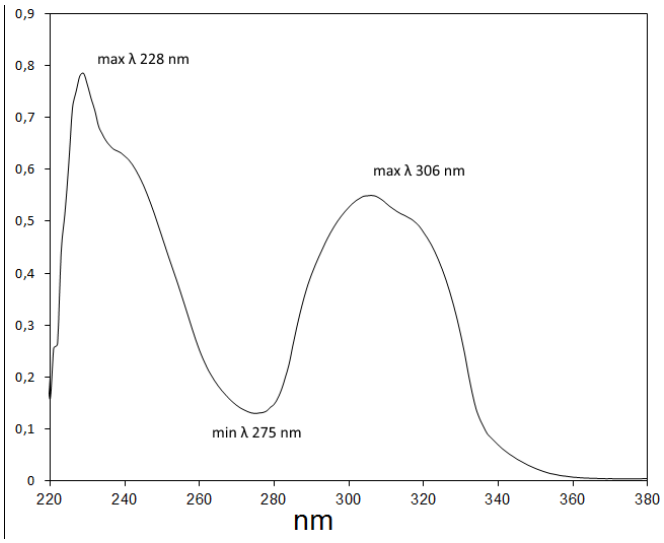

UV spectrum of **9**

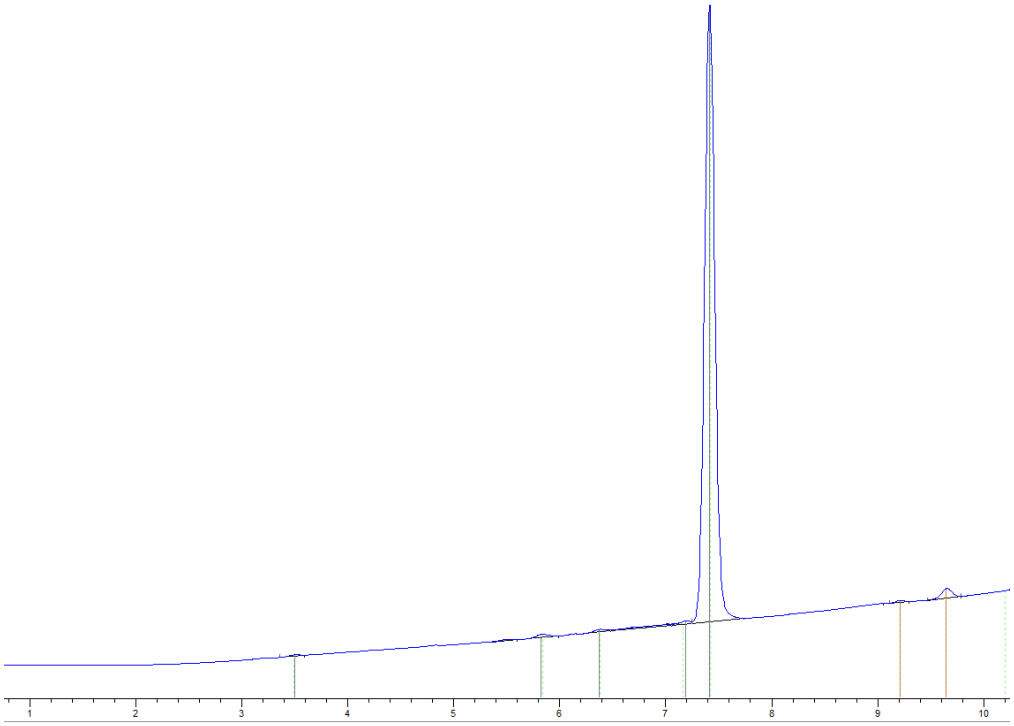

Analytical HPLC of **9**

***Octyl (N-(4-(benzofuran-2-yl)-2-methoxyphenyl)sulfamoyl)carbamate* (2)**

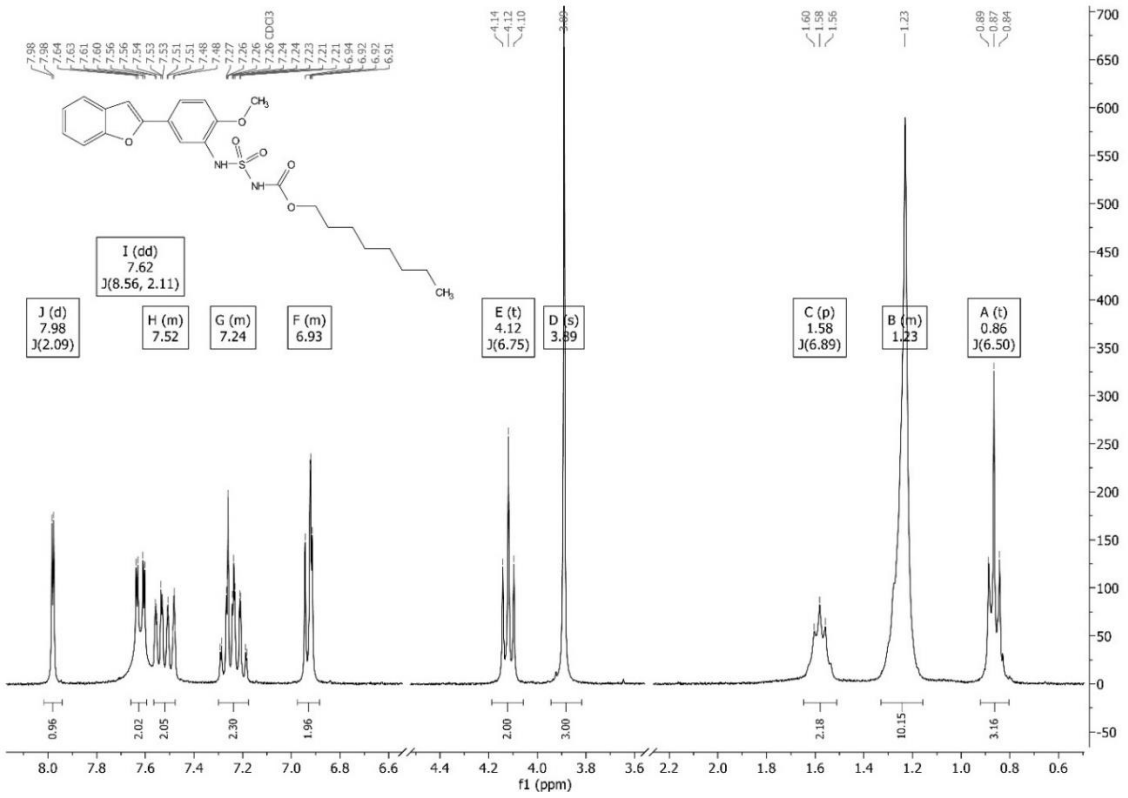

^{1}H NMR spectrum of **2**

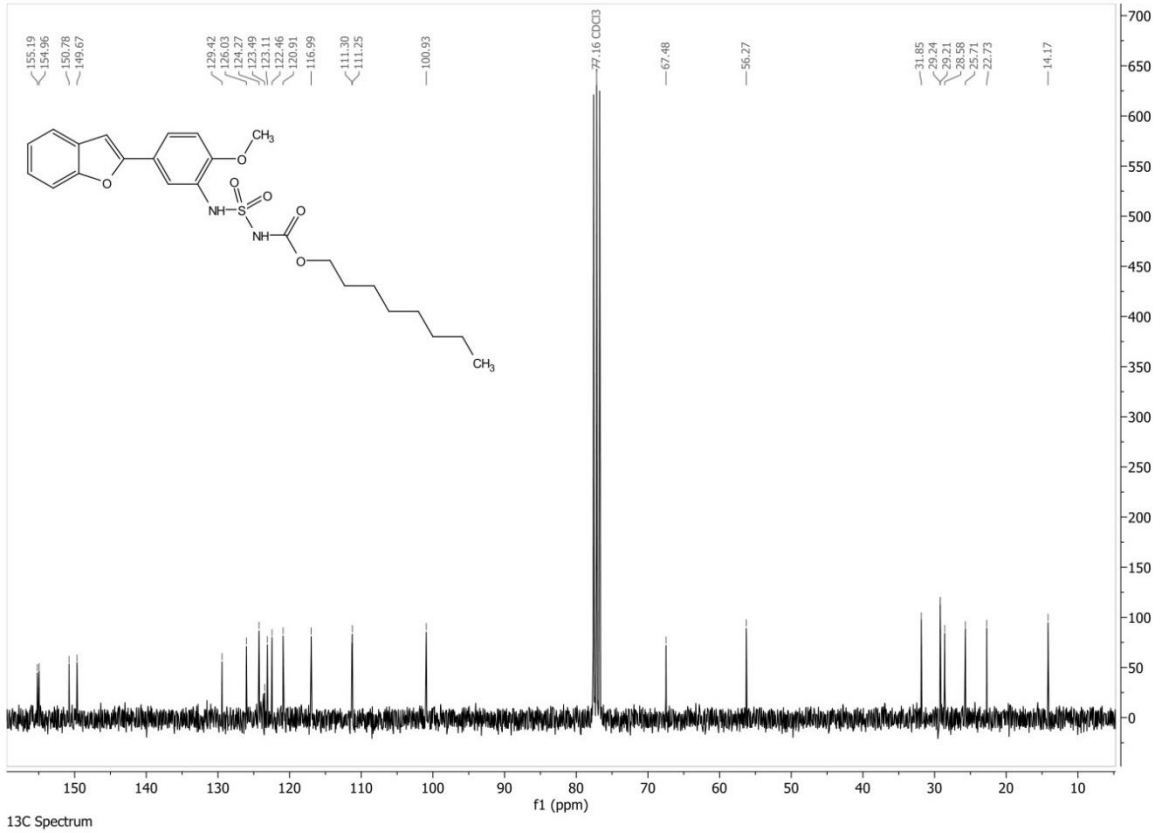

^{13}C NMR spectrum of **2**

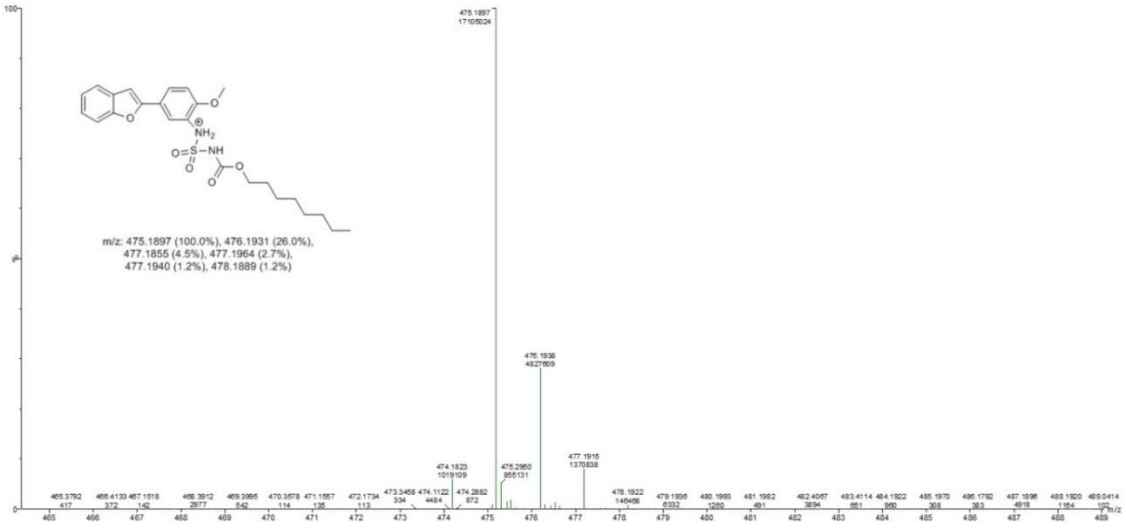

HRMS spectrum of **2**

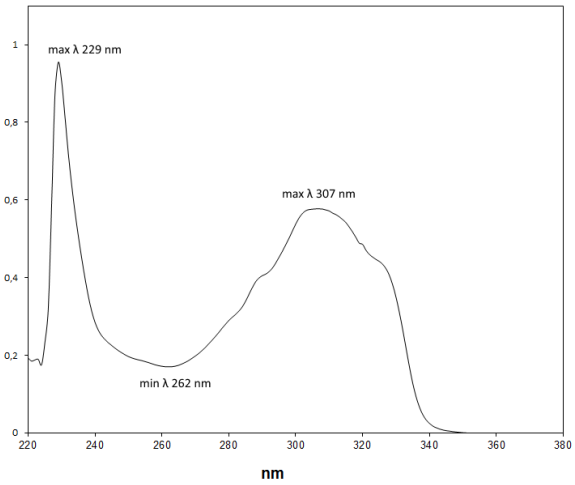

UV spectrum of **2**

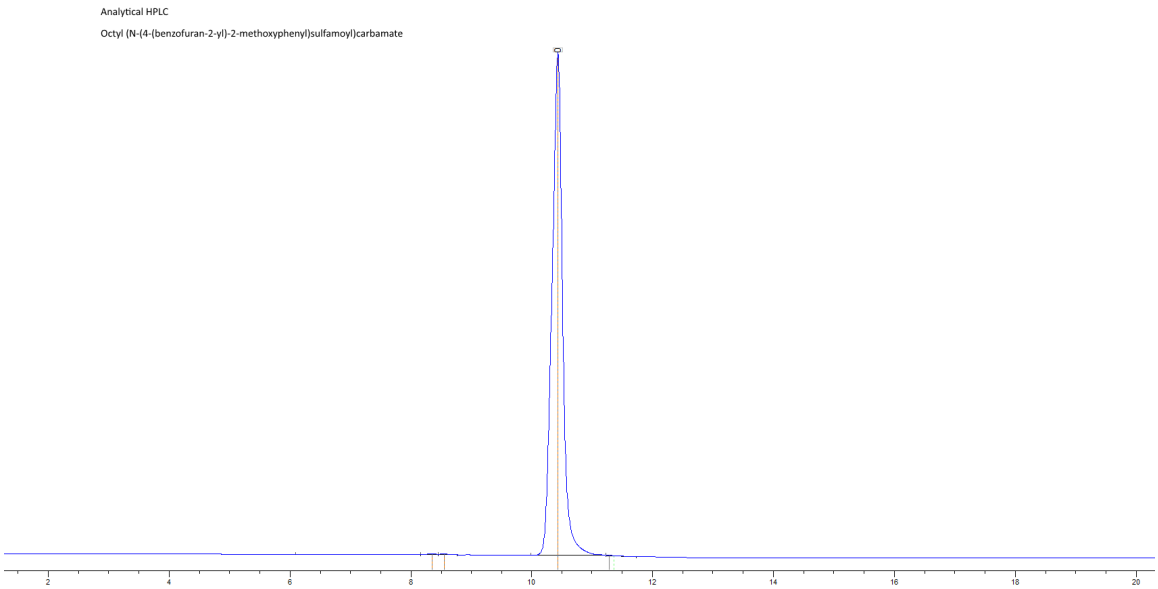

Analytical HPLC of **2**

3-methoxy-4-nitrobenzoyl chloride (11)

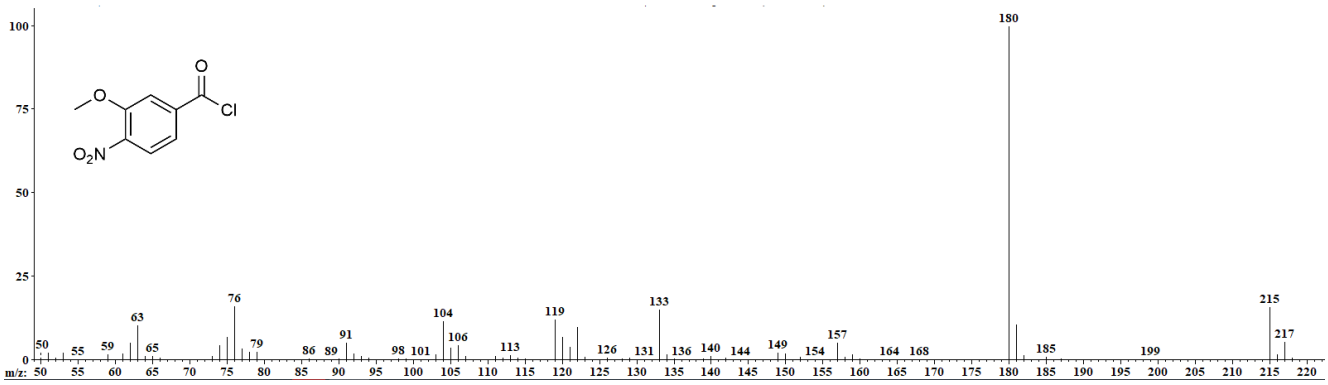

MS spectrum of **11**

N,3-dimethoxy-N-methyl-4-nitrobenzamide **(12)**

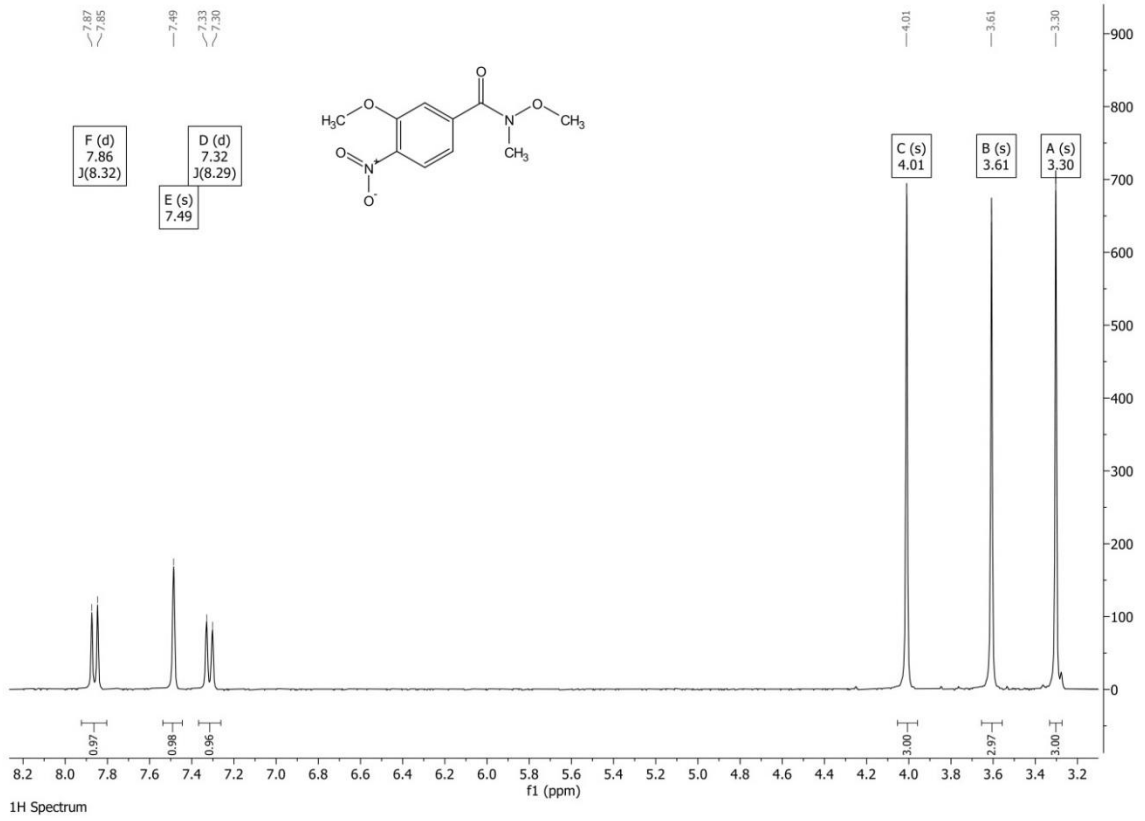

[1]H NMR spectrum of **12**

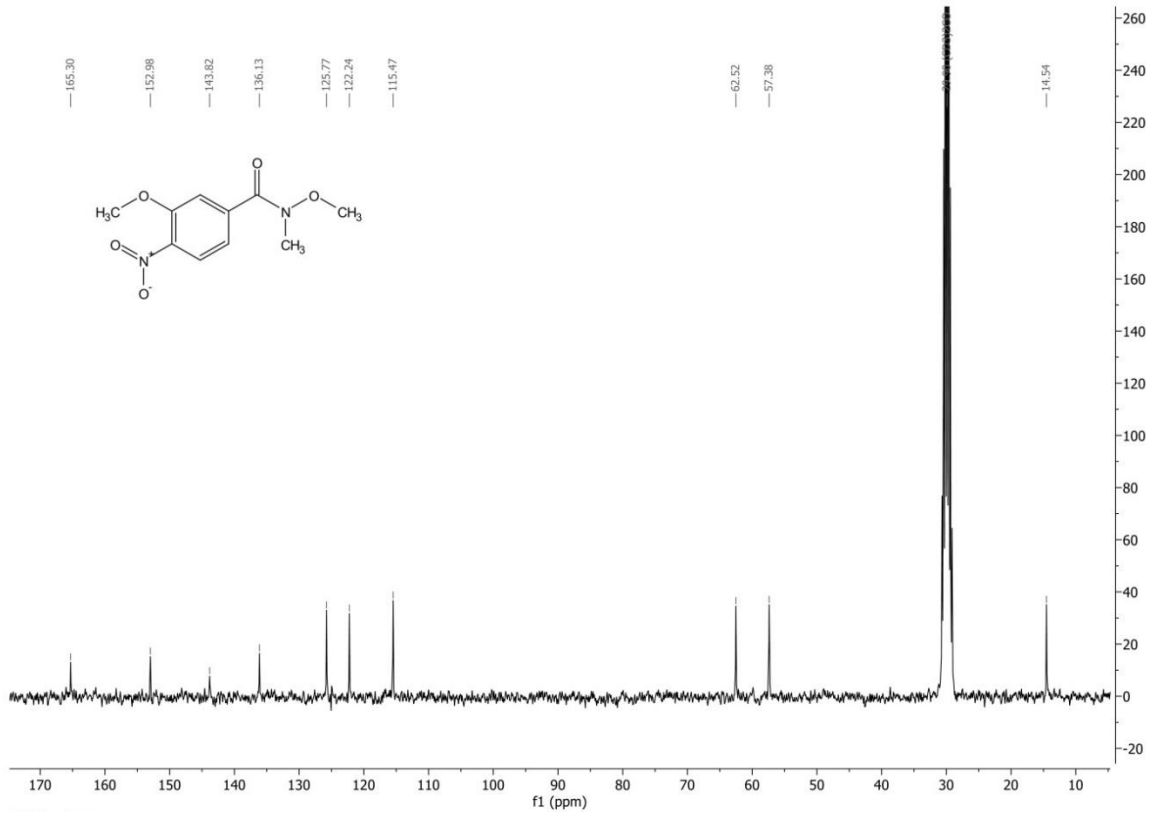

[13]C NMR spectrum of **12**

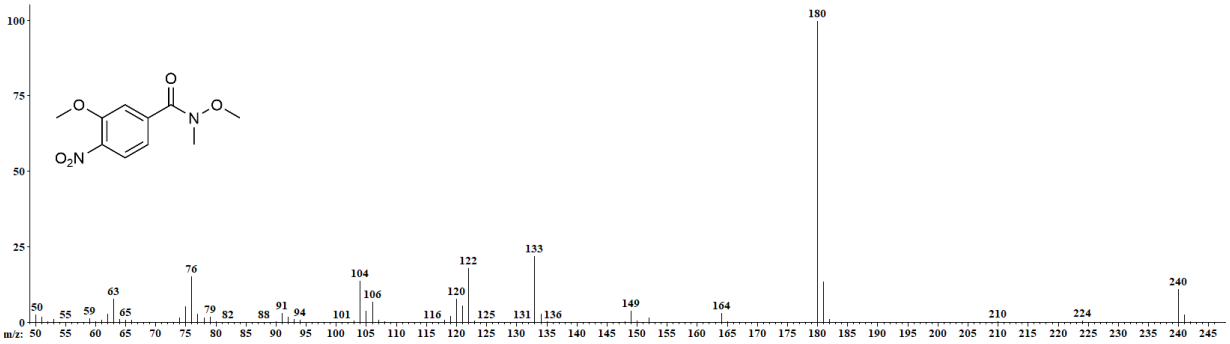

MS spectrum of **12**

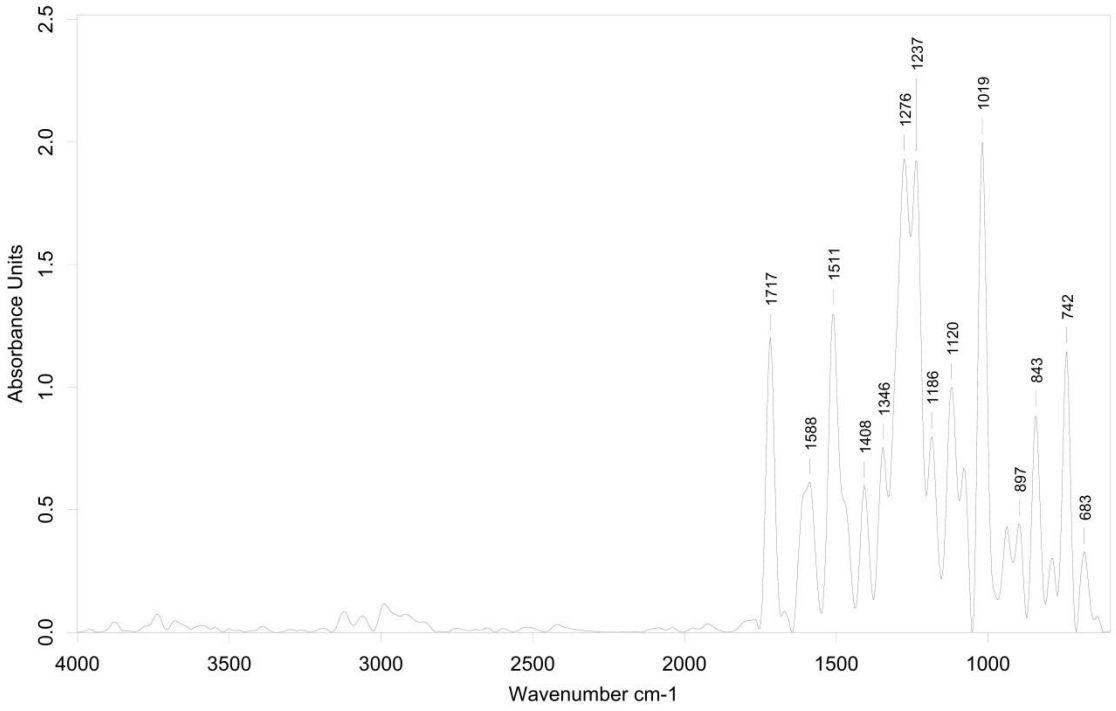

IR spectrum of **12**

1-(3-methoxy-4-nitrophenyl)ethan-1-one **(15)**

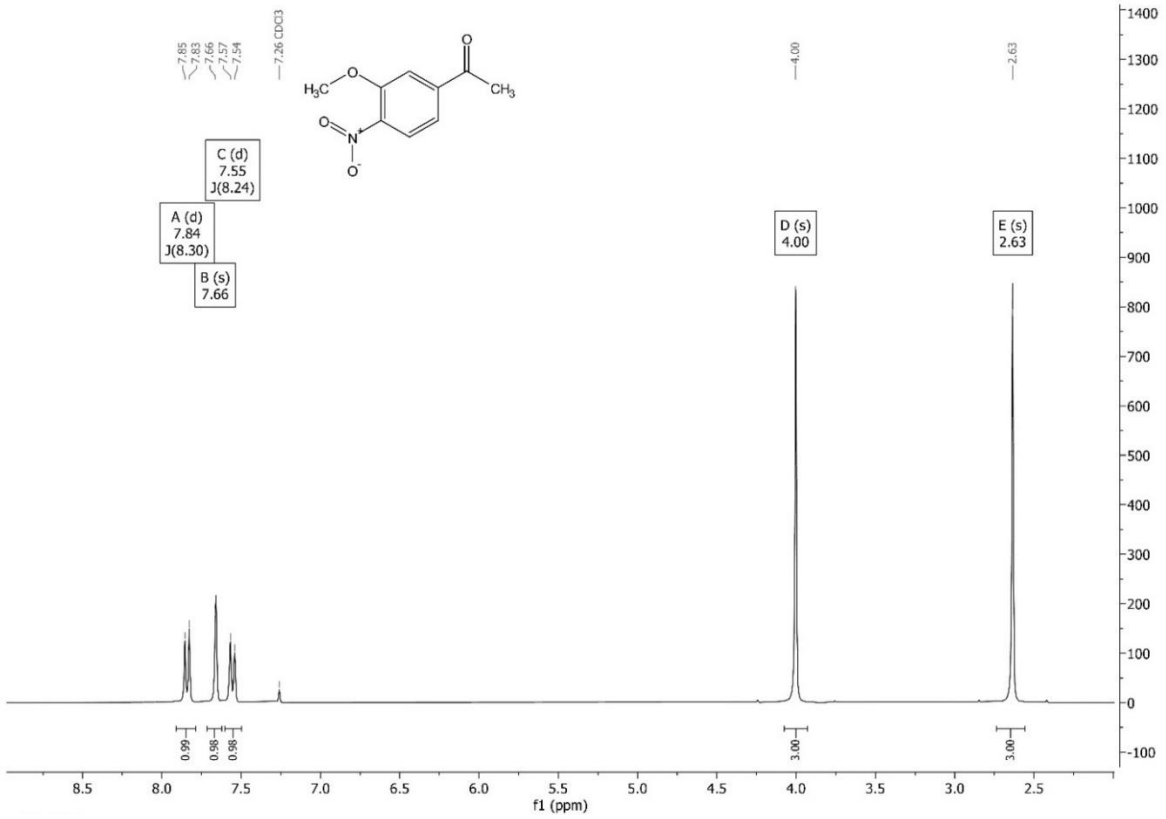

^{1}H NMR spectrum of **15**

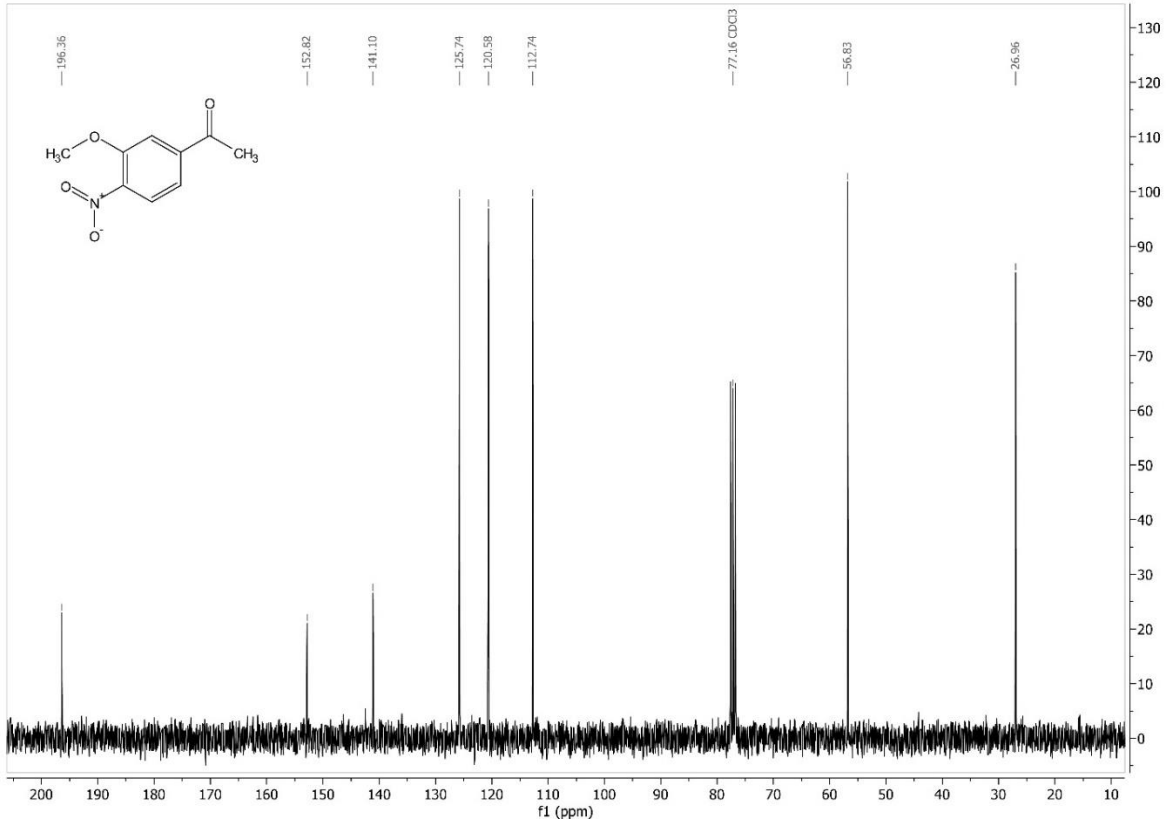

^{13}C NMR spectrum of **15**

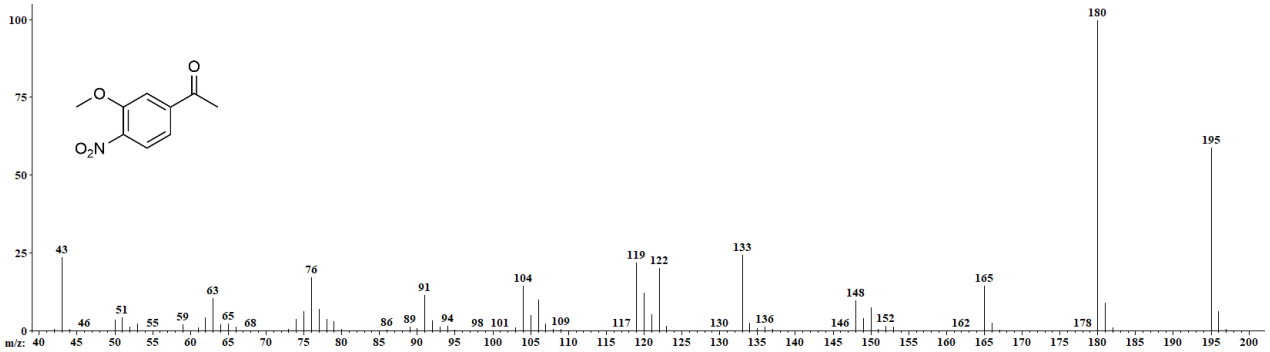

MS spectrum of **15**

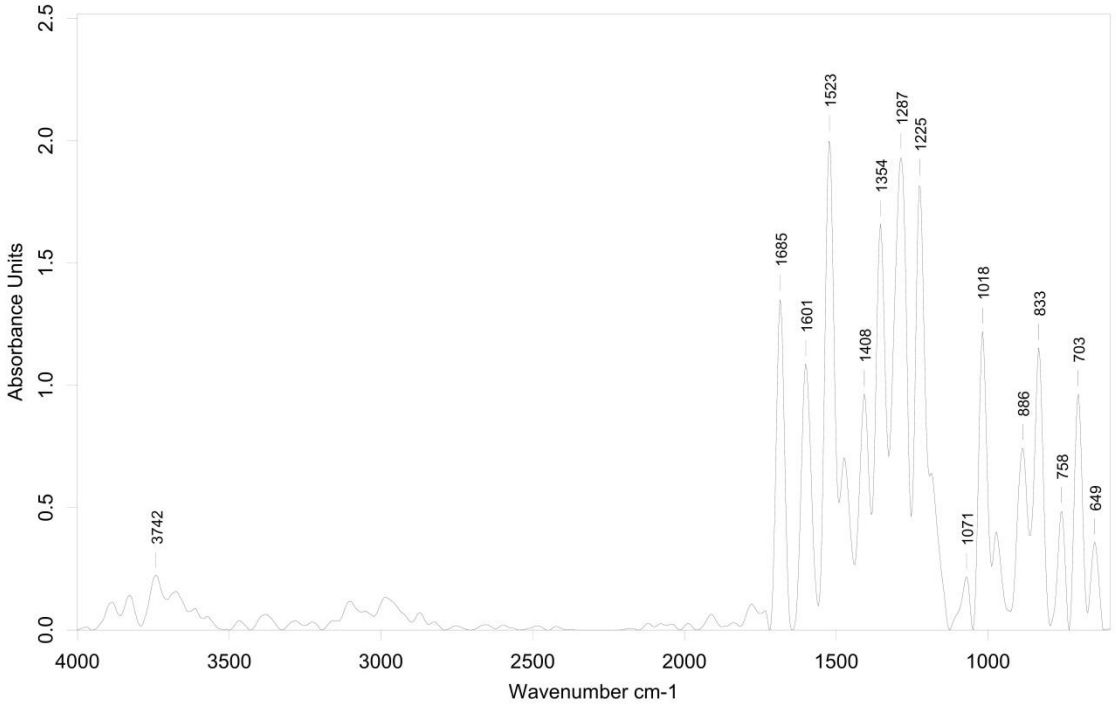

IR spectrum of **15**

1-(4-amino-3-methoxyphenyl)ethan-1-one **(16)**

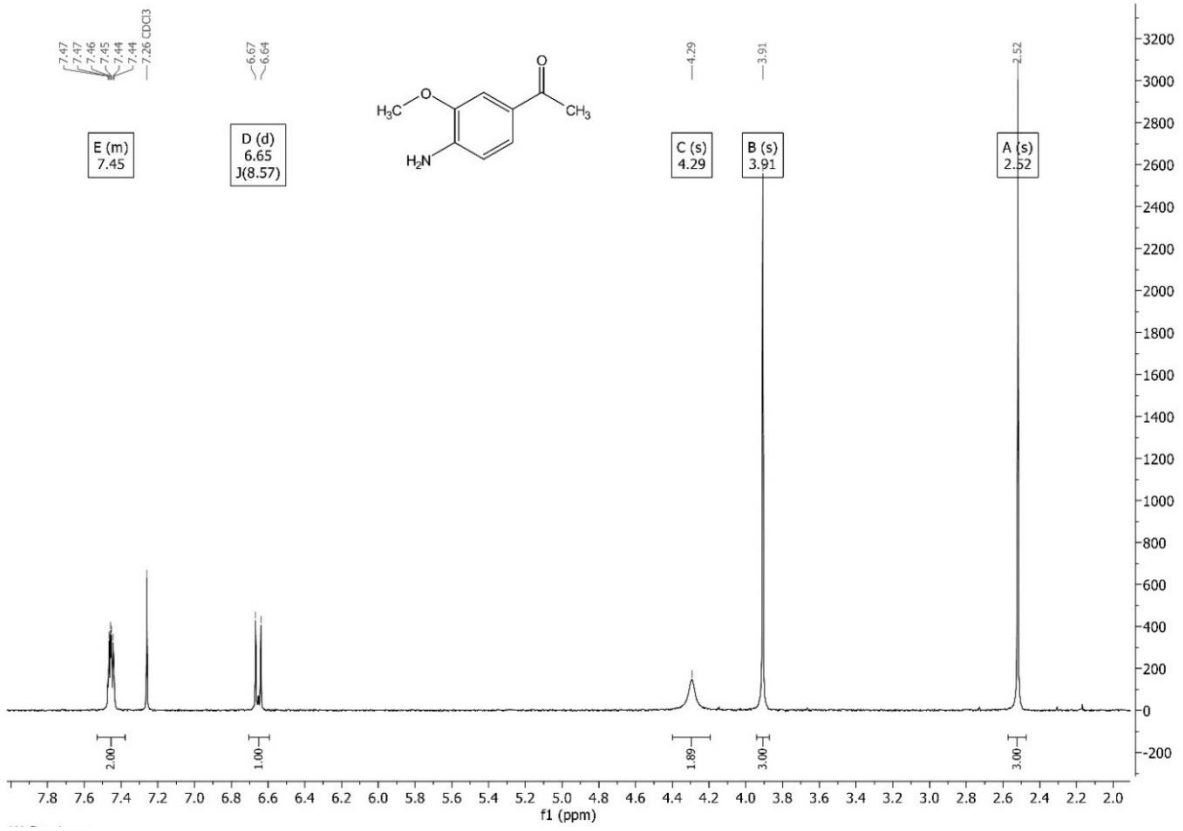

[1]H NMR spectrum of **16**

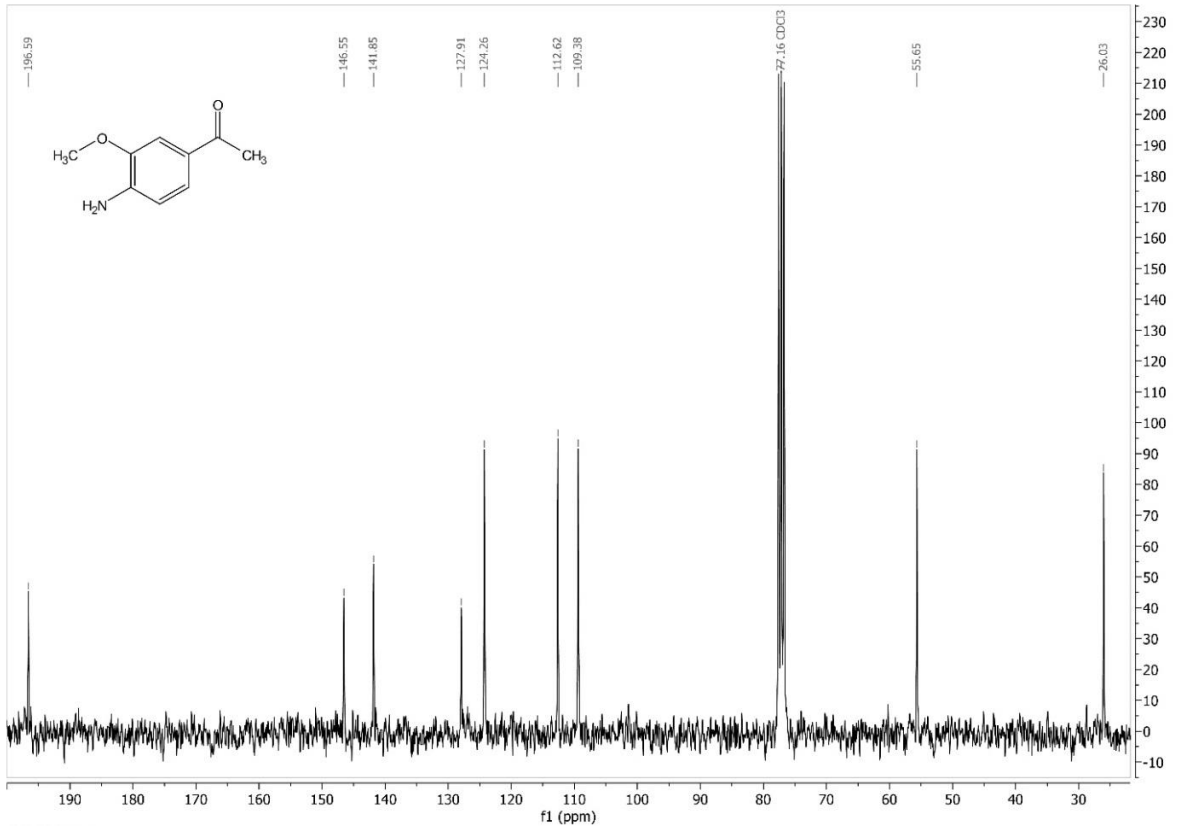

[13]C NMR spectrum of **16**

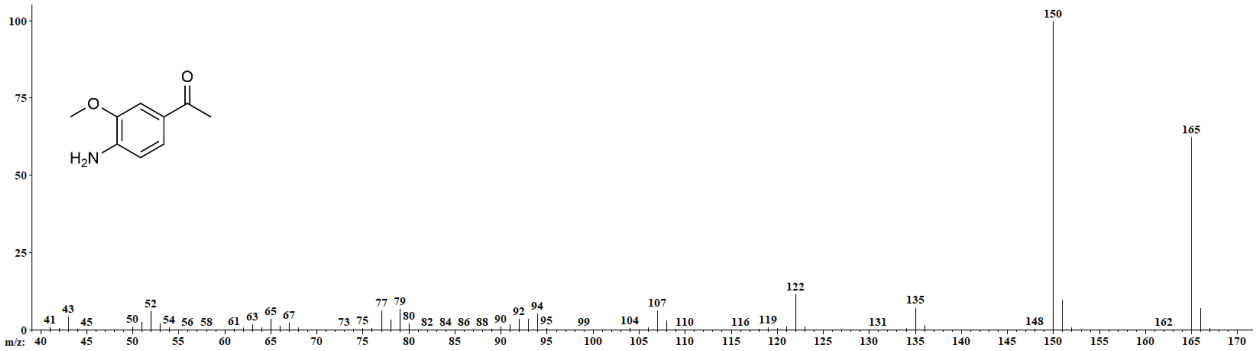

MS spectrum of **16**

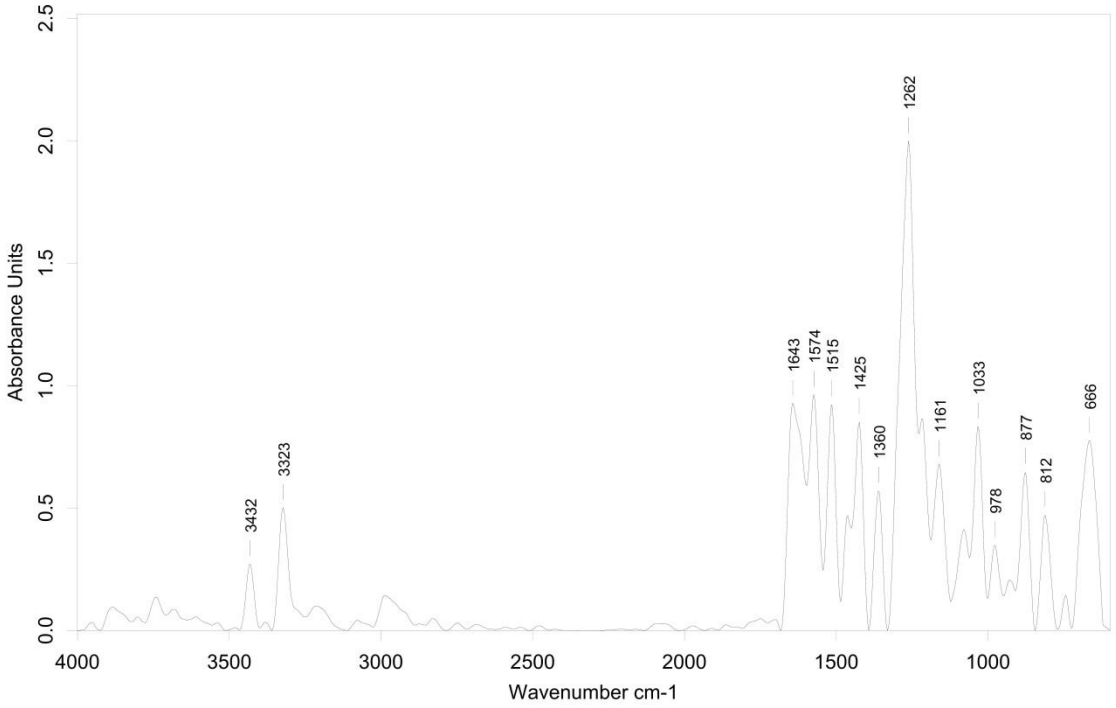

IR spectrum of **16**

***4-(1H-indol-2-yl)-2-methoxyaniline* (17)**

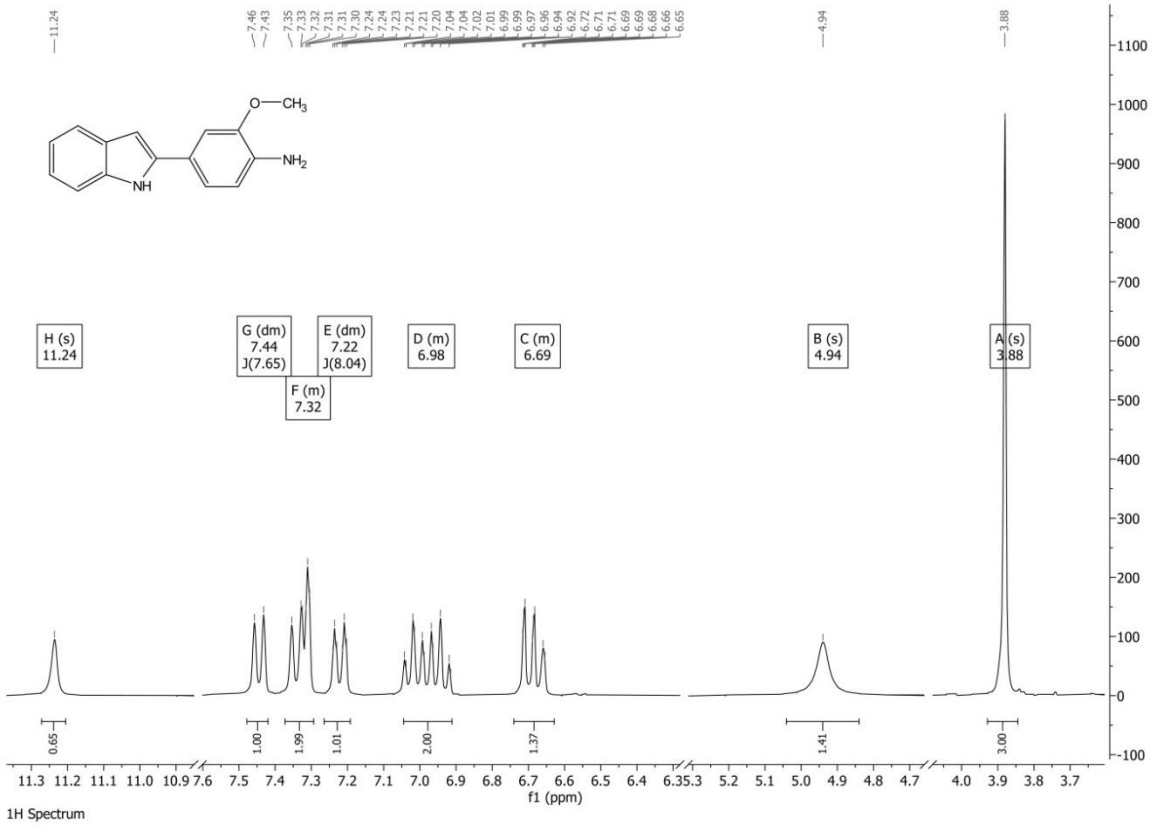

[1]H NMR spectrum of **17**

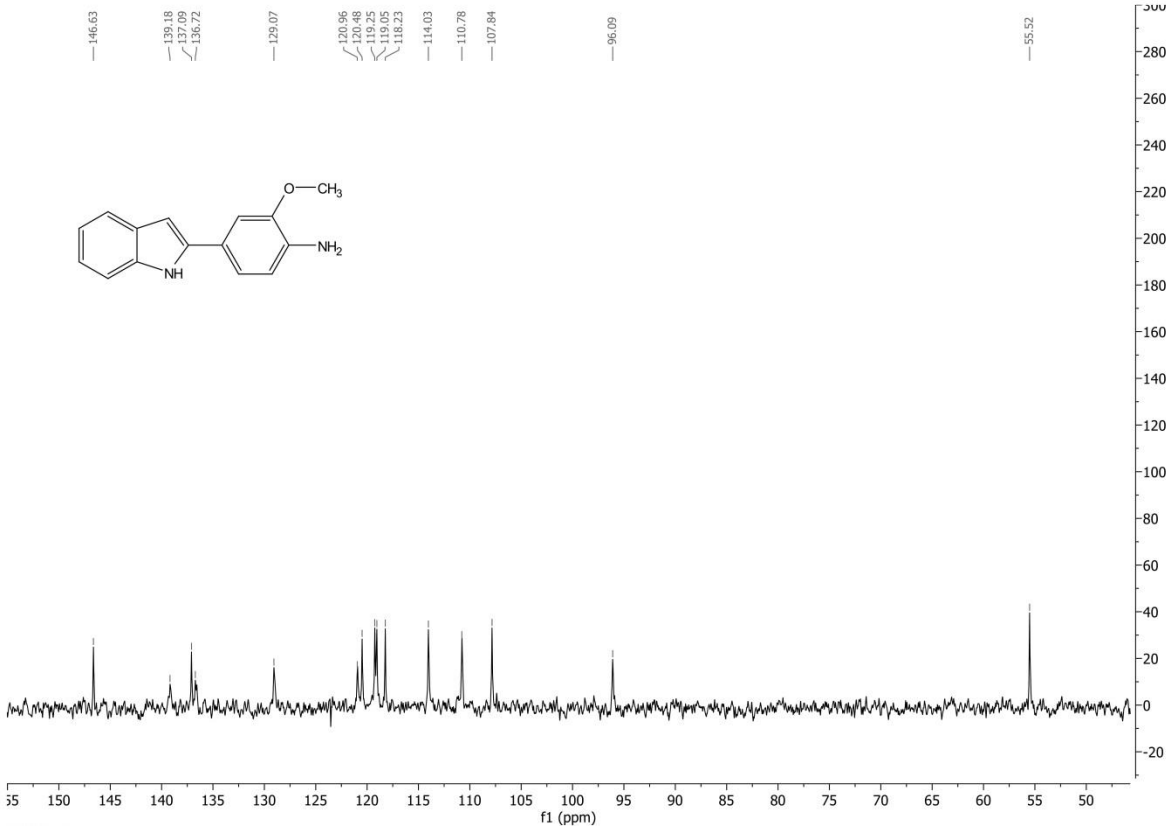

[13]C NMR spectrum of **17**

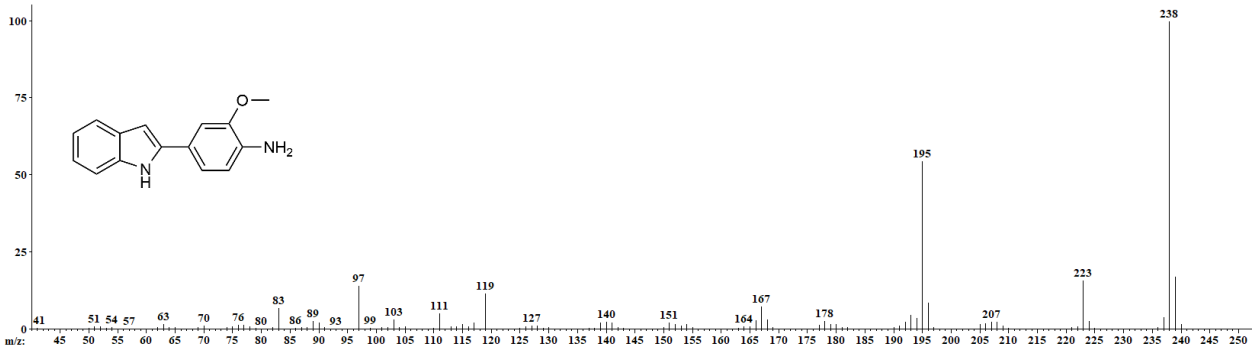

MS spectrum of **17**

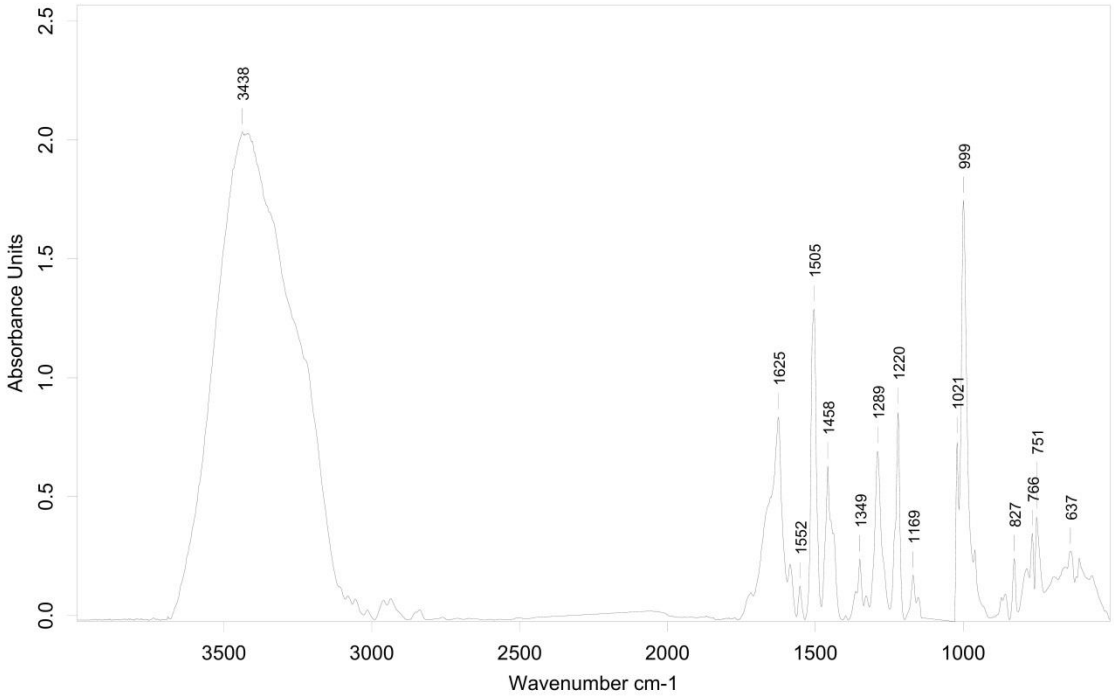

IR spectrum of **17**

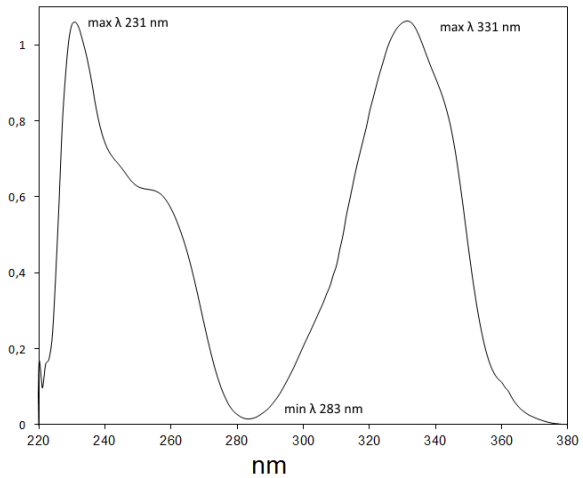

UV spectrum of **17**

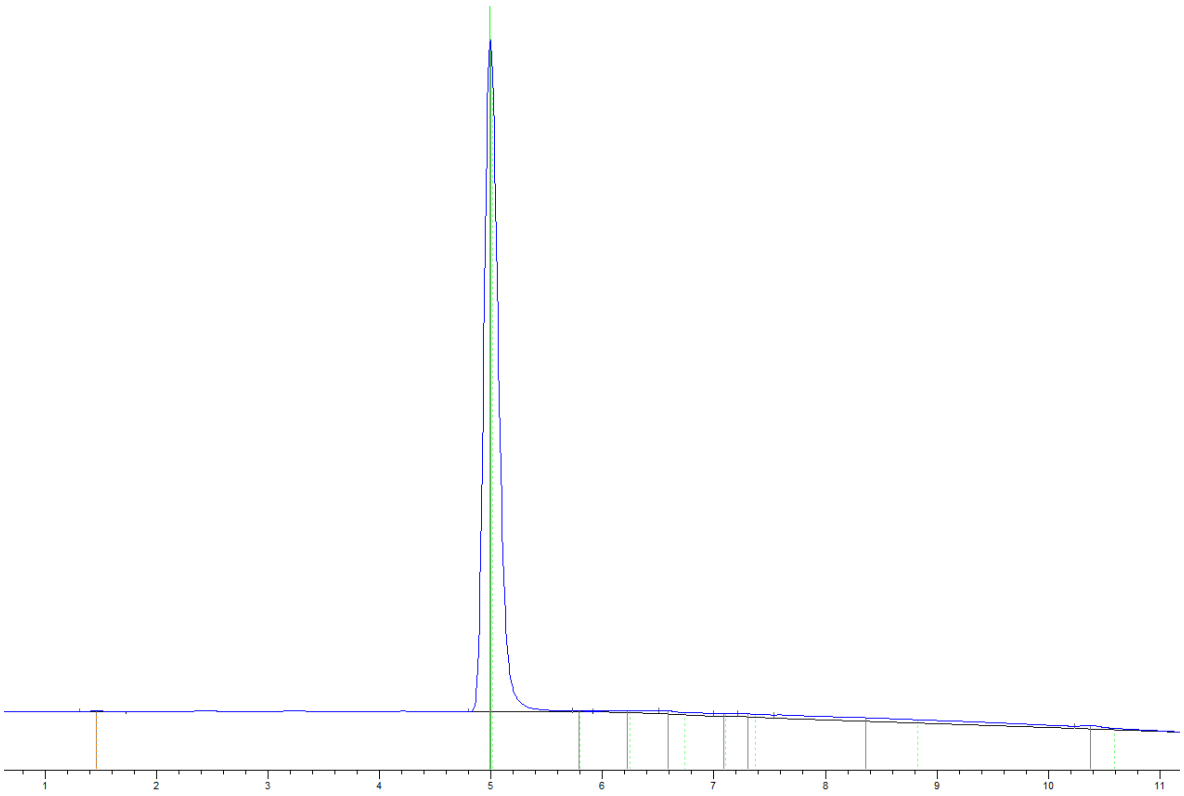

Analytical HPLC of **17**

***Octyl (N-(4-(1H-indol-2-yl)-2-methoxyphenyl)sulfamoyl)carbamate* (3)**

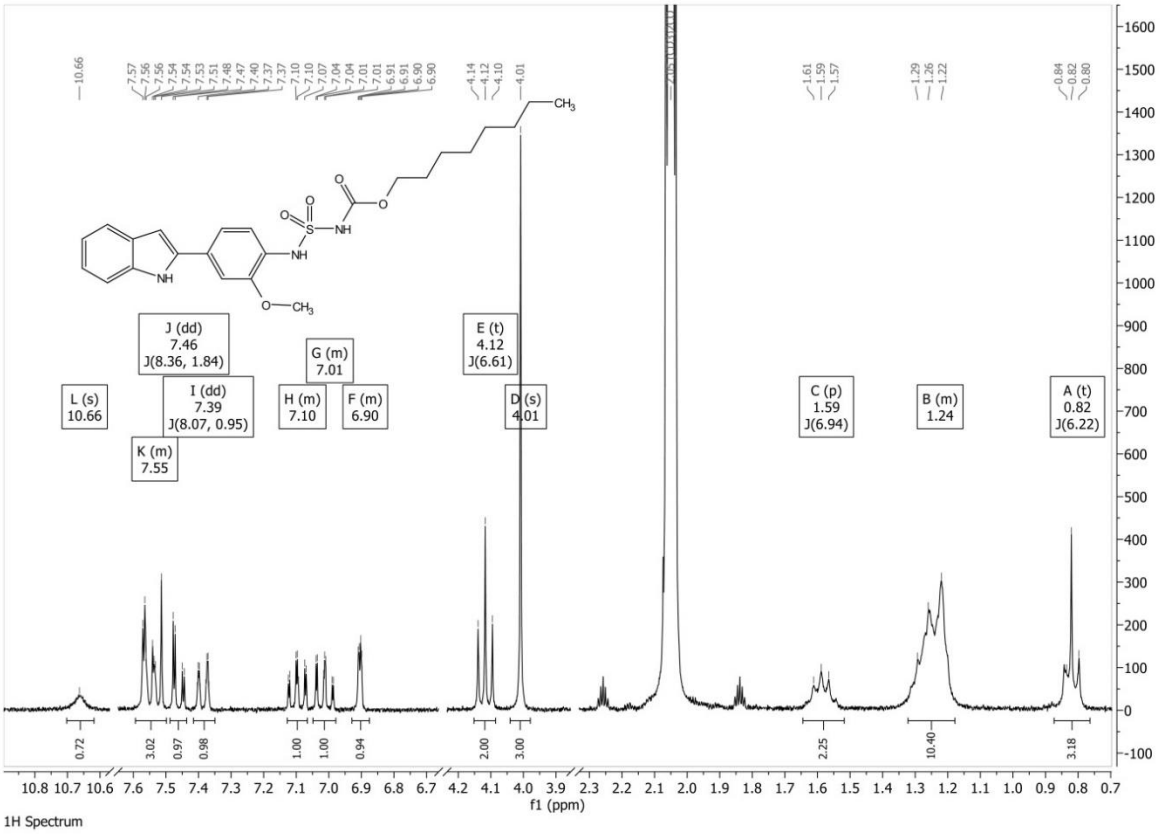

[1]H NMR spectrum of **3**

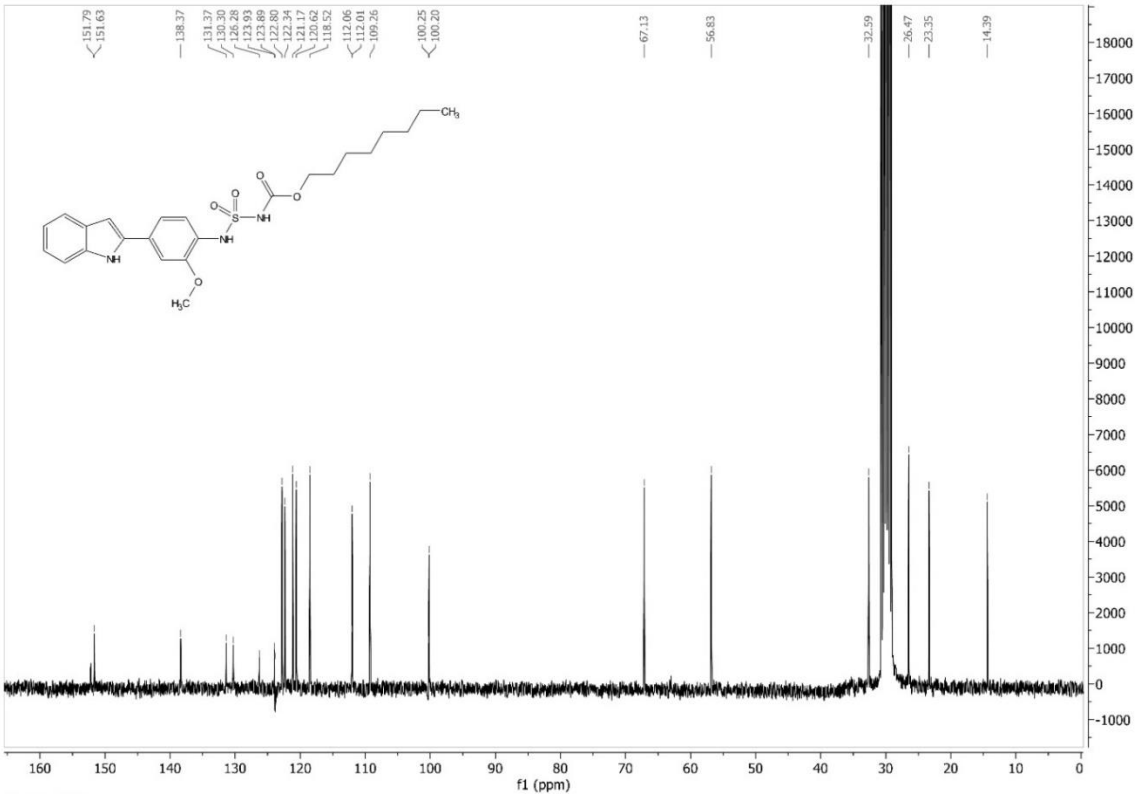

[13]C NMR spectrum of **3**

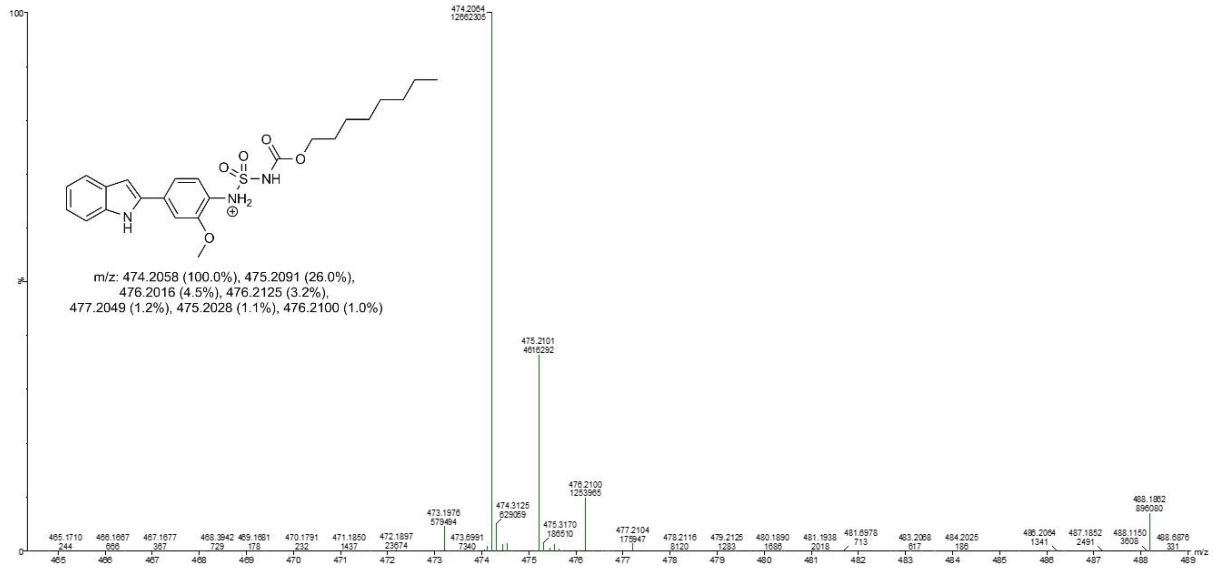

HRMS spectrum of 3

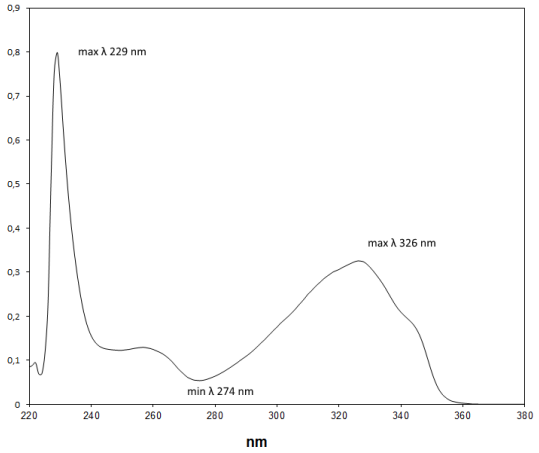

UV spectrum of **3**

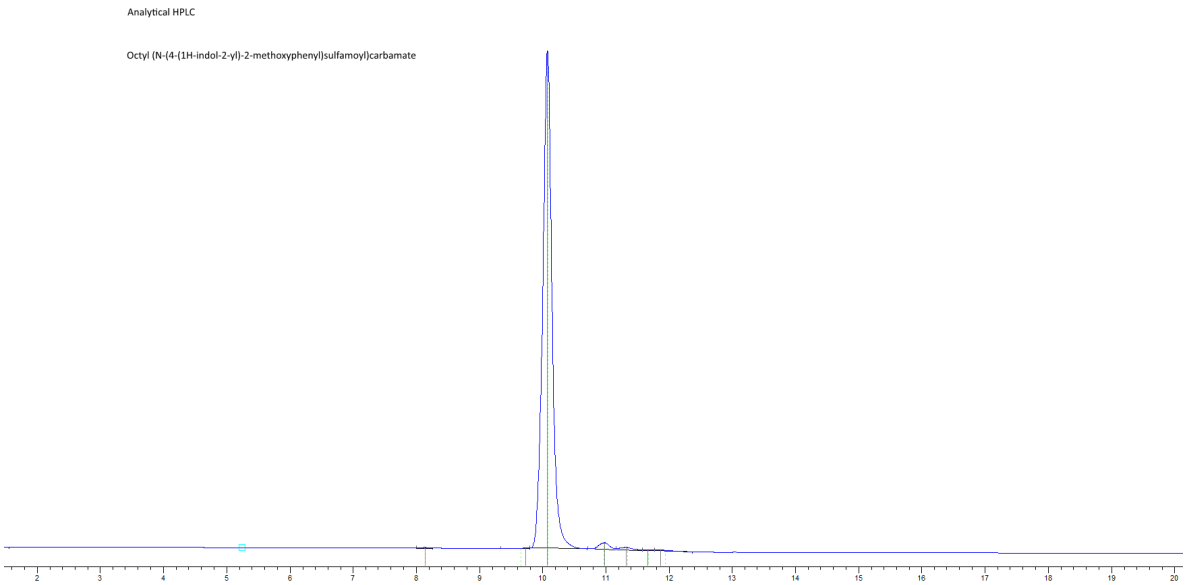

Analytical HPLC of **3**

Analysis of the docking binding modes of compound 3 represented in Figures 4A and 4C:

Complex 3(1):ALOX15

The 2-phenylindole ring is located inside the cavity of monomer A, but not as deeply as in 8b, which is likely due to the new relative position of the OCH_3 group. This group now points in the opposite direction to that in 8b (toward Gly407 and not Phe175). As always, both the sulfonamide and the hydrophobic tail are located at the entrance to the cavity.

Summary of the most relevant interactions:

• H-bonding between the NH group of the 2-phenylindole ring and the oxygen atom of the Ile400 backbone (d(0109-H5-O-Ile400) = 1.945 Å).

• The NH_2 group of Asn193 of monomer B forms a H bond with one of the oxygen atoms of the sulfonamide (d(0109-O2-HD22-Asn193)=3.213 Å) and interacts electrostatically with the OCH_3 group (d(0109-O1-HD22-Asn193)=4.377 Å) and the ester group as a whole (d(0109-O4-HD22-Asn193)=3.103 Å; d(0109-O5-HD22-Asn193)=3.409 Å).

• The NH group of the sulfonamide closest to the ring system forms an H bond with the backbone oxygen atom of Leu192 of monomer B (d(0109-H13-O-Leu192(B)) = 1.887 Å).

• Arg403 establishes an H bond with one of the sulfonamide oxygen atoms (d(0109-O3-HH11-Arg403) = 1.691 Å) and a favorable electrostatic interaction with the NH group of the sulfonamide closest to the ring system (d(0109-N2-HH12-Arg403) = 3.428 Å).

Complex 3(2):ALOX15

This pose would be equivalent to that of 8b, although the orientation of the OCH_3 group obviously changes. Specifically, this group is oriented toward the interior of the cavity, but now points toward Ile663 and would be located on the C-terminus of helix α18 of monomer A, instead of pointing toward Phe175 and helix α2 of interface monomer A.

Summary of the most relevant interactions:

• The NH of the 2-phenylindole ring exhibits an unfavorable electrostatic interaction with the OH group of the Fe-OH_2+ cofactor (d(0109-H5-HO-Fe) = 2.084 Å) and a large number of hydrophobic interactions with residues at or near the bottom of the cavity, specifically with Leu358, Leu362, Leu408, Val409, Phe415, and Leu597.

• The OCH_3 group interacts electrostatically with the side chain of Gln596, establishing a favorable interaction with the NH2 group (d(0109-O1-HE22-Gln596)=3.273 Å) and an unfavorable interaction with the keto group (d(0109-O1-OE1-Gln596)=3.041 Å), and Arg599 establishes a favorable electrostatic interaction with one of its NH_2 groups (d(0109-O1-HH21-Arg599)=3.967 Å).

• One of the sulfonamide oxygen atoms forms an H bond with the NH_2 group of the side chain of Gln596 (d(0109-O1-HE22-Gln596)=1.321 Å).

• The NH group of the sulfonamide furthest from the ring system forms an H bond with the O group of the backbone of Arg403 (d(0109-H14-O-Arg403)=2.133 Å).

• The ester group forms an H bond through its keto oxygen atom with the side chain of Arg403 (d(0109-O4-HH11-Arg403)=1.600 Å) and two favorable electrostatic interactions through the other oxygen atom, one with the NH_2 group of the side chain of Asn193 of monomer B (d(0109-O5-HD22-Arg403)=3.446 Å) and another with the NH_2 group of the side chain of Asn406 (d(0109-O5-HD21-Arg403)=3.921 Å).